International Journal of Bifurcation and Chaos, Vol. 12, No. 10 (2002) 2175–2207

GLOBAL BIFURCATIONS OF BASINS IN A TRIOPOLY GAME

ANNA AGLIARI
Istituto di Econometria e Matematica,
Università Cattolica del Sacro Cuore,
Largo Gemelli, 1, 20123 Milano, Italy
aagliari@mi.unicatt.it

LAURA GARDINI
University of Urbino, Italy
gardini@econ.uniurb.it

TONU PUU
University of Umea, Sweden
tonu.puu@econ.umu.se

Received August 3, 2001; Revised October 2, 2001

A Cournot model based on bounded inverse demand function and constant marginal production costs is studied. The case of three producers is considered and the adjustment process reduces to a three-dimensional noninvertible map in the output of competitors. The analysis of the dynamical behavior of the map is performed by the "critical curve method", extended to the critical surfaces in 3D. By this method, we explain the different bifurcations in the basins of attraction and in the attracting sets. In particular, given the economic application, feasible trajectories are focused, starting from the simple situation of two identical producers and extending the results to the generic case.

Keywords: Three-dimensional map; basin bifurcations; critical surfaces; subcritical Neimark bifurcation.

1. Introduction

Elementary textbook economics considers two opposite market forms: perfect competition and monopoly. In perfect competition a large number of producing firms face an equally large number of consumers. Such an atomistic firm cannot influence market price, and so takes it as a given datum. The monopolist, on the contrary, alone faces the numerous consumers, and can make maximum profit by deliberately reducing supply so as to establish the monopoly price which maximizes its profits. For this, it must know how market demand varies with the price it charges.

A contextually intermediate case is oligopoly, with just a few suppliers facing the many consumers on the demand side, but it is analytically more complex than either of the extreme cases. The oligopolist has the power to influence price noticeably, but it must have the information the monopolist has about demand, and further conjecture how the competitors react to its own actions.

Oligopoly theory is one of the oldest branches of mathematical economics, and its basic model was formulated by Augustin Cournot in 1838 already [Cournot, 1838]. Cournot oligopoly assumes that the firms use quantity as their strategic variable of action. This assumption was severely

criticized in 1883 by Joseph Bertrand and others [Bertrand, 1883; Edgeworth, 1897], who suggested that price and not quantity should be the strategic variable. The argument was that if the commodity really were homogenous, as implied by the quantity adjustment procedure, then one competitor could throw the others out by any infinitesimal undercutting of prices. Though several interesting variants of oligopoly theory emerged from this criticism, the Cournot model was later reestablished as the core of oligopoly theory. Other developments were connected with the assumptions about strategic behavior. Notable were Heinrich von Stackelberg's 1938 contribution about leadership/followership [von Stackelberg, 1938], and Ragnar Frisch's of 1933 on conjectural variations [Frisch, 1933]. Cournot's original assumption — that each competitor assumes the others to retain their last moves even though observing the contrary — had seemed rather simplistic. However, it must be admitted that Cournot's original assumptions, even in this respect, produced a more interesting offspring than the more sophisticated revisions ever did.

In 1978 Rand [1978], suggested oligopoly games as an example for dynamical economic systems which easily lead to complex dynamics and hinted at several possibilities to attain this. The probably simplest assumptions under which this occurs, i.e. iso-elastic demand and constant though different marginal costs for the competitors, were suggested by one of the present authors in 1991 [Puu, 1991], for the case of two competitors. A period-doubling cascade to chaos was in fact observed. Three competitors add further scenarios, such as Neimark–Hopf bifurcations.

In the 1930s several demand functions, mainly of the kinked straight line type, were tried, and such phenomena as coexistent attractors and unending oscillations were noted, see [Palander, 1936] and [Wald, 1936]. However, the iso-elastic demand function, meaning that the quantity demanded by the consumers is reciprocal to its price, has the advantage that it arises from very basic microeconomic theory. If the consumers maximize some utility function of the Cobb–Douglas type, the most often used assumption, then they spend given fractions of their incomes on each commodity. This also holds true for aggregate demand of the market, being the sum of the demand of all the individuals, maybe all different fractions of different incomes, but also all reciprocal to price.

The authors tried their hands on such a model with three competitors in a previous publication, [Agliari *et al.*, 2000; Puu, 2000]. However, the iso-elastic demand function, though well rooted in economic principles has a certain drawback in the oligopoly context. As price and quantity are reciprocal, their product, i.e. total sale values for a monopolist, is a constant. Accordingly, a collusive oligopoly (though normally forbidden by law in most countries), which behaves as a single monopolist, could retain the total income but reduce costs to zero by producing nothing and letting price go to infinity. This a bit academic, but the annoying problem can be avoided by letting price be reciprocal to the total quantity supplied plus some positive constant, whose reciprocal then establishes a maximum price.

The study of such a model is the object of the present paper. The three-dimensional model will be described in Sec. 2 and, as often occurs in dynamic games, we shall get a three-dimensional noninvertible map whose dynamic behavior will be considered in the consecutive sections. The study is mainly devoted to the determination in the four-dimensional parameter space of the economically meaningful region of the model and of the feasible region in the state space.

As we shall see, reasonable ranges for the parameters may be associated with unfeasible trajectories or meaningful dynamics. Their evolutions as the parameters are changed will be explained by the theory of critical surfaces and contact bifurcations between basin boundaries and critical surfaces. As described in the basic references [Gumonwski & Mira, 1980a, 1980b; Mira *et al.*, 1996; Abraham *et al.*, 1997], the critical surfaces (or manifolds), the three-dimensional analogous of critical lines and critical points in maps of dimensions two and one, respectively, give a powerful method to study the global dynamical properties of a noninvertible map. Thus, following this theory, we are able to detect the global bifurcations which cause qualitative changes in the structure of the region of feasible trajectories, leading to the creation of volumes with a complex topological structure.

The plan of the work is as follows. After the description of the general model in Sec. 2, a simpler map in Sec. 3, is introduced depending only on three parameters and topologically conjugated to the previous one. The regions of interest both for the mathematical system (admissible trajectories and regions) and for the economic application

(feasible trajectories and regions) are also defined and the local stability analysis of the unique Cournot equilibrium point is performed. Section 4 is devoted to the study of the properties of the model in the particular case of two producers with identical marginal costs: in particular, local stability and feasibility analysis of the fixed point are given as well as the study of the critical sets of the map. The dynamical behaviors of the model in this particular case are described in Secs. 5 and 6. More precisely, in Sec. 5 we study the geometrical structure of the admissible and feasible regions when the Cournot equilibrium point is the unique attracting set of the map. We show some contact bifurcations in the feasible region which cause changes in the connected convex region (Sec. 5.2) and transitions to connected, not convex, and disconnected regions (Sec. 5.3). Section 6 is related to the study of the more complex dynamics of the map due to a global bifurcation of "saddle-node type", after which the map exhibits a multistability situation, and to a Neymark–Hopf bifurcation of subcritical type, after which the Cournot equilibrium point is no longer attracting. The effects of such bifurcations on the feasible region are also investigated. Finally, in Sec. 7, we return to the generic model and the analysis performed in the previous sections help us to understand the dynamical properties of the model with different marginal costs. The paper is closed with two Appendices: in the first one we give some topics related to game theory and the definition of reaction function, useful to understand the derivation of the model for the not expert readers. In the second Appendix the proof of the local stability and feasibility of the fixed point in the case of two identical producers is reported.

2. The Model

As in [Agliari *et al.*, 2000] we consider a Cournot triopoly but now we assume that the inverse demand function, i.e. the price as a function of the demanded quantity, is given by

$$p = \frac{1}{q + W} \tag{1}$$

where p is the unit price of the commodity and q is the demanded quantity.

W in (1) is the reciprocal of the maximum price obtainable and it has to be considered as a positive parameter.

Assuming for each producer the production cost proportional to the output, we denote with a, b and c the *constant marginal costs*, i.e.

$$\begin{aligned} C_1(x) &= ax \\ C_2(y) &= by \\ C_3(z) &= cz \end{aligned}$$

are the cost functions for the three producers, respectively, where x, y and z denote the supplies. At equilibrium, the total supply equals the demanded quantity, that is $q = x + y + z$, and the profit functions U_i, $i = 1, 2, 3$, i.e. the difference between the revenue and the costs, are given by

$$\begin{aligned} U_1 &= \frac{x}{x + y + z + W} - ax \\ U_2 &= \frac{y}{x + y + z + W} - by \\ U_3 &= \frac{z}{x + y + z + W} - cz \end{aligned} \tag{2}$$

By (2), the reaction functions of the players are easily obtained, and depend on the expected supplies x^e, y^e and z^e of the competitors. More precisely, the reaction function of the player i depends on the production of the other two producers, as follows (see Appendix A for details):

$$\begin{aligned} r_1(y^e, z^e) &= \sqrt{\frac{y^e + z^e + W}{a}} - y^e - z^e - W \\ r_2(x^e, z^e) &= \sqrt{\frac{x^e + z^e + W}{b}} - x^e - z^e - W \\ r_3(x^e, y^e) &= \sqrt{\frac{x^e + y^e + W}{c}} - x^e - y^e - W \end{aligned} \tag{3}$$

Assuming a one-stage game with the assumption that the players have perfect foresight about the moves of the competitors, the solution of the game is the *Cournot equilibrium point*, the intersection point of the reaction functions (3). Thus the Cournot equilibrium point is given by the solution of the system

$$\begin{cases} x = \sqrt{\dfrac{y + z + W}{a}} - y - z - W \\ y = \sqrt{\dfrac{x + z + W}{b}} - x - z - W \\ z = \sqrt{\dfrac{x + y + W}{c}} - x - y - W \end{cases} \tag{4}$$

Some algebraic manipulations show that the system (4) has only one solution

$$E^* = \begin{pmatrix} \dfrac{(b+c-a)(1+\sqrt{1+W(a+b+c)}) - aW(a+b+c)}{(a+b+c)^2} \\ \dfrac{(a-b+c)(1+\sqrt{1+W(a+b+c)}) - bW(a+b+c)}{(a+b+c)^2} \\ \dfrac{(a+b-c)(1+\sqrt{1+W(a+b+c)}) - cW(a+b+c)}{(a+b+c)^2} \end{pmatrix} \tag{5}$$

and the Cournot equilibrium of the game is unique.

So, if the producers are full rational players, their production choices are given respectively by the components of E^* in (5) and the market is in equilibrium. But, if we relax the hypothesis of perfect rationality the market changes, because the players move according to their expectations, adjusting at each stage their production, and only after a suitable number of moves, if ever, the game will be in equilibrium. In our work we consider this last situation and we suppose, with Cournot, that the producers adjust their production simultaneously and that they have *naive expectations* on the choices of their competitors, i.e. they assume that at the stage t the production by the other players will be the same as in the previous stage. These assumptions lead to an adjustment process described by the discrete dynamical system

$$T : \begin{cases} x' = \sqrt{\dfrac{y+z+W}{a}} - y - z - W \\ y' = \sqrt{\dfrac{x+z+W}{b}} - x - z - W \\ z' = \sqrt{\dfrac{x+y+W}{c}} - x - y - W \end{cases} \tag{6}$$

where the symbol $'$ denotes the unit time advancement operator (i.e. if (x, y, z) represents the vector of choices at time t, then (x', y', z') gives the choices at time $(t+1)$).

Observe that the point E^* in (5) is the unique fixed point of the map T.

The study of the dynamical properties of (6) as well as its local and global bifurcations, shall be the aim of the following sections of the paper. In particular we study the Cournot equilibrium point (5) as an attractive fixed point for the map T and its basin of attraction. Another important question to which we shall give an answer, is about the coexistence of other attractors with the Cournot equilibrium, and the asymptotic behavior of the adjustment process when the Cournot equilibrium is not attracting.

3. Dynamical Properties of the Adjustment Process

Let us first rewrite our model (the map T) in a more suitable form, making use of the following result:

Proposition 1. *The dynamics of the map T in (6) with parameters (a, b, c, W) and that of $(\tau a, \tau b, \tau c, W/\tau)$ with $\tau > 0$ are topologically conjugate, via the homeomorphism $\phi(x, y, z) = (\tau x, \tau y, \tau z)$.*

Proof. The proof follows trivially by calculating $\phi^{-1}(T(\phi(x, y, z)))$, where ϕ^{-1} is the inverse of ϕ, i.e. $\phi^{-1}(x, y, z) = (1/\tau)(x, y, z)$. ■

Given Proposition 1, we can consider the normalization with respect to a marginal cost, say a, considering as parameters $(1, b/a, c/a, aW) = (1, h, k, v)$ and study the properties and the dynamics of the map by varying the three parameters (h, k, v). The range of interest of the "reduced parameters" in this formulation is $h \geq 0$, $k \geq 0$ and $v \geq 0$. Moreover, if we assume the marginal cost a to be the highest marginal cost, we have the constraints $0 \leq h \leq 1$, $0 \leq k \leq 1$ and $0 \leq v \leq 1$, where the hypothesis $v \leq 1$ assures that all the producers have marginal cost smaller than the maximum price obtainable. We note that taking $W = 0$ the model reduces to the case analyzed in [Agliari *et al.*, 2000], and the reduced parameters h and k have the same meaning as the parameters introduced in that paper.

3.1. *The model with the reduced parameters* $(1, h, k, v)$

Let us consider the normalization of the parameters as described above, so that the map we are

interested in becomes

$$T:\begin{cases} x' = \sqrt{y+z+v} - (y+z+v) \\ y' = \sqrt{\dfrac{x+z+v}{h}} - (x+z+v) \\ z' = \sqrt{\dfrac{x+y+v}{k}} - (x+y+v) \end{cases} \tag{7}$$

which we shall continue to denote by T, for the sake of simplicity, being the reduced form that we consider in this work (that is, more rigorously, the two maps (6) and (7) are topologically conjugated, following Proposition 1 with $\tau = 1/a$).

It is clear that the applicative model is meaningful only for positive values of the variables x, y and z, and in particular, the fixed point is "admissible" iff all the components are positive. Moreover it is immediate to see that the map T is not defined in the whole three-dimensional space. The natural domain of definition of T is the region, say D, given by the set of points (x, y, z) which satisfy:

$$D = \{(y+z+v) \geq 0,\ (x+z+v) \geq 0,\ (x+y+v) \geq 0\} \tag{8}$$

But we have to consider a "repeated" game, and thus we are interested in a subset of this set, which we call S, which consists of the points (x, y, z) for which we have $T^n(x, y, z) \in D$ for any $n \geq 0$. We shall call *admissible* such points and trajectories in S. However, not all the admissible trajectories are meaningful, so we restrict our interest to a lower set, which we call *feasible*, denoted as F, and made up by positive trajectories. Formally: the locus of admissible points for which $T^n(x, y, z) \in S \cap R^3_+$ for any $n \geq 0$. We shall call *unfeasible* the other points and trajectories in S.

$$S = \{(x, y, z) \in D : T^n(x, y, z) \in D \text{ for any } n \geq 0\}$$

$$F = \{(x, y, z) \in S : T^n(x, y, z) \in S \cap R^3_+ \text{ for any } n \geq 0\}$$

Obviously $F \subseteq S \subseteq D$.

The existence (and structure) of such a trapping region F of feasible trajectories is not easy to ascertain. We can be sure of its existence when the map T has an attracting (i.e. asymptotically stable) set belonging to R^3_+ (fixed point or something else), and we shall see how it may be determined.

Let us start studying the simpler situation of the attracting fixed point, belonging to F.

The fixed point of T in (7) is given by:

$$E^* = \begin{pmatrix} x^* \\ y^* \\ z^* \end{pmatrix} = \begin{pmatrix} \dfrac{(h+k-1)(1+\sqrt{1+v(h+k+1)}) - v(1+h+k)}{(h+k+1)^2} \\ \dfrac{(1+k-h)(1+\sqrt{1+v(h+k+1)}) - vh(1+h+k)}{(h+k+1)^2} \\ \dfrac{(1+h-k)(1+\sqrt{1+v(h+k+1)}) - vk(1+h+k)}{(h+k+1)^2} \end{pmatrix} \tag{9}$$

E^* belongs to the positive orthant of the space if the following conditions are satisfied

$$\begin{cases} (h+k-1)(1+\sqrt{1+v(h+k+1)}) - v(1+h+k) > 0 \\ (1+k-h)(1+\sqrt{1+v(h+k+1)}) - vh(1+h+k) > 0 \\ (1+h-k)(1+\sqrt{1+v(h+k+1)}) - vk(1+h+k) > 0 \end{cases} . \tag{10}$$

Conditions (10) can be rewritten as

$$\begin{cases} (1+h+k) - 2 > \dfrac{v(1+h+k)}{1+\sqrt{1+v(1+h+k)}} \\ (1+h+k) - 2h > \dfrac{v(1+h+k)}{1+\sqrt{1+v(1+h+k)}}\, h \\ (1+h+k) - 2k > \dfrac{v(1+h+k)}{1+\sqrt{1+v(1+h+k)}}\, k \end{cases}$$

that is

$$\begin{cases} 1+h+k > 1+\sqrt{1+v(1+h+k)} \\ \dfrac{1+h+k}{h} > 1+\sqrt{1+v(1+h+k)} \\ \dfrac{1+h+k}{k} > 1+\sqrt{1+v(1+h+k)} \end{cases} \tag{11}$$

Now, we need to obtain the following

Proposition 2. *If $h \in (0, 1]$ and $k \in (0, 1]$ then the Cournot equilibrium point belongs to the positive orthant of R^3 iff*

$$h+k > 1+v \tag{12}$$

In particular a necessary condition for $E^* \in R^3_+$ is

$$v > 1 \tag{13}$$

Proof. Assuming $h \in (0, 1]$ and $k \in (0, 1]$, the last two inequalities in (11) are satisfied once the first one holds,

$$1+h+k > 1+\sqrt{1+v(1+h+k)}$$

from which, by standard algebraic manipulation, we get (12).

Moreover, from $v < h+k-1$, $h \le 1$ and $k \le 1$, we obtain $v < 1$. ■

Proposition 2 has an immediate economic meaning: the adjustment process gives feasible trajectories only if the maximum price obtainable ($P = 1/W$) is greater than the marginal costs of the producers. In fact if the parameters of the map are normalized with respect to the maximum marginal cost a, we assume $v = aW < 1$, i.e. $P > a$. Observe also that feasible trajectories can be obtained only if $h + k > 1$, i.e. $b + c > a$.

Otherwise, if we relax the assumptions on the marginal costs, and assume that $h > 1$ and/or $k > 1$, i.e. the parameters of the map are not normalized with respect to the maximum marginal cost, for the positivity of E^* a condition similar to (13) can be obtained, that is v smaller than the maximum marginal cost. In fact, if k is the maximum marginal cost, in (11) we have to consider

$$\frac{1+h+k}{k} > 1+\sqrt{1+v(1+h+k)}$$

which gives

$$v < \frac{1+h-k}{k^2} \le \frac{1}{k}$$

Observe that the last condition always implies $P > c$, i.e. the maximum price obtainable must be greater than the marginal costs.

In the following we shall assume $0 < k \le h \le 1$ and $v \le 1$.

Let us now study the local stability of the fixed point. As usual, we have to consider the Jacobian matrix of the map T, which is given by

$$J(x, y, z) = \begin{bmatrix} 0 & -\dfrac{1}{2}\dfrac{-1+2\sqrt{y+z+v}}{\sqrt{y+z+v}} & -\dfrac{1}{2}\dfrac{-1+2\sqrt{y+z+v}}{\sqrt{(y+z+v)}} \\ -\dfrac{1}{2}\dfrac{-1+2\sqrt{(x+z+v)h}}{\sqrt{(x+z+v)h}} & 0 & -\dfrac{1}{2}\dfrac{-1+2\sqrt{(x+z+v)h}}{\sqrt{(x+z+v)h}} \\ -\dfrac{1}{2}\dfrac{-1+2\sqrt{(x+y+v)k}}{\sqrt{(x+y+v)k}} & -\dfrac{1}{2}\dfrac{-1+2\sqrt{(x+y+v)k}}{\sqrt{(x+y+v)k}} & 0 \end{bmatrix} \tag{14}$$

and evaluating the Jacobian matrix (14) in E^*, we obtain the matrix

$$J^* = \begin{bmatrix} 0 & A & A \\ B & 0 & B \\ C & C & 0 \end{bmatrix} \tag{15}$$

where

$$A = \frac{(1+h+k) - 2(1+\sqrt{1+v(1+h+k)})}{2(1+\sqrt{1+v(1+h+k)})} \qquad B = \frac{(1+h+k) - 2h(1+\sqrt{1+v(1+h+k)})}{2h(1+\sqrt{1+v(1+h+k)})}$$

$$C = \frac{(1+h+k) - 2k(1+\sqrt{1+v(1+h+k)})}{2k(1+\sqrt{1+v(1+h+k)})}$$

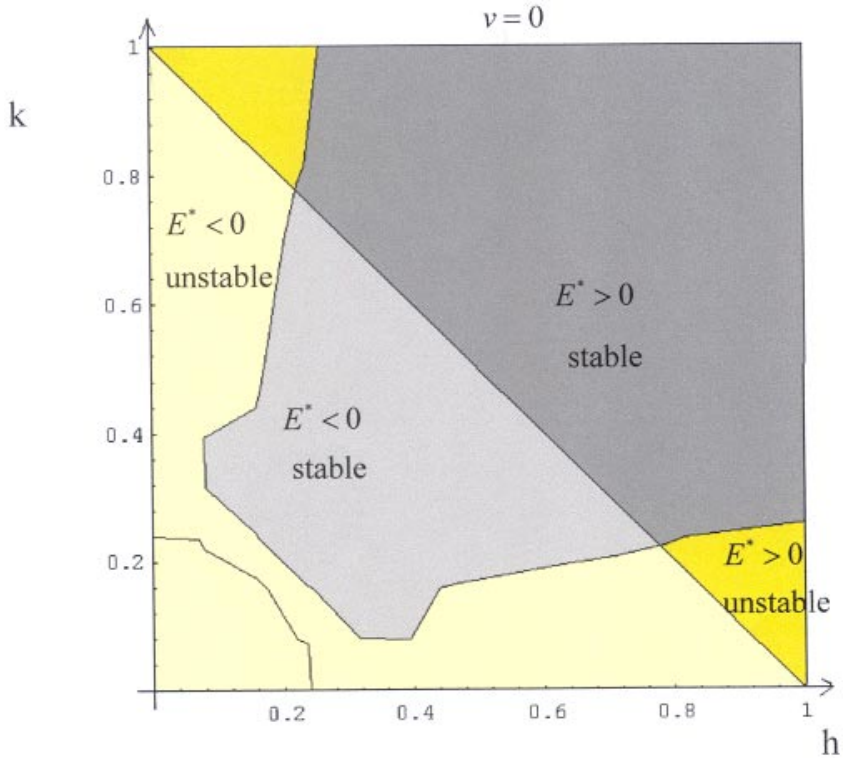

(a)

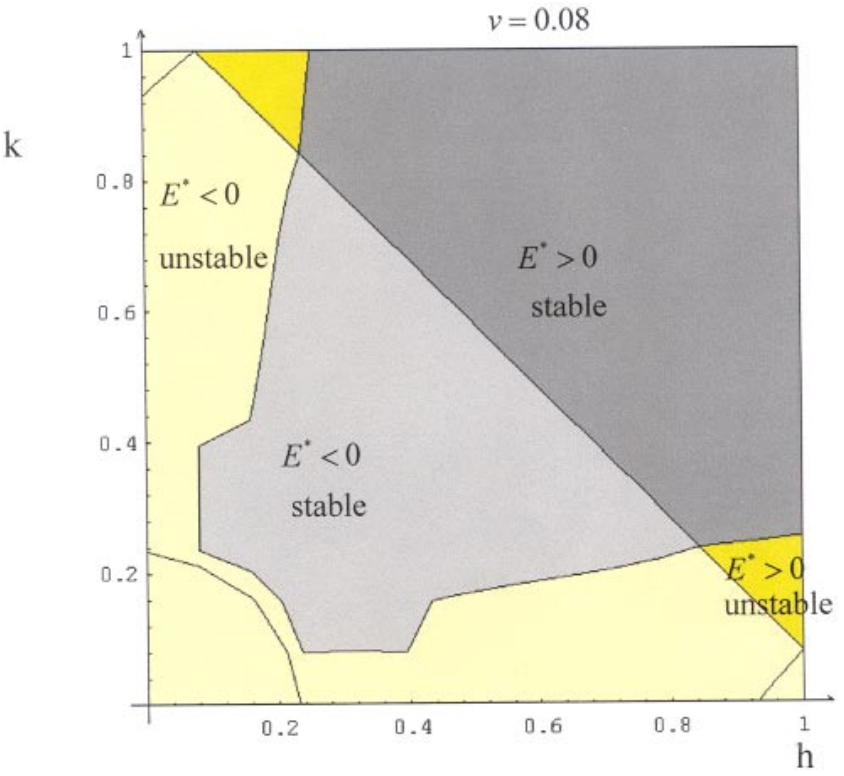

(b)

Fig. 1. Stability regions for the fixed point E^* in the parameter space (h, k), obtained at different values of v. In the dark gray region E^* is stable with positive coordinates and in the dark yellow region E^* is unstable with positive coordinates. The curve separating the two regions is a Neimark–Hopf bifurcation curve.

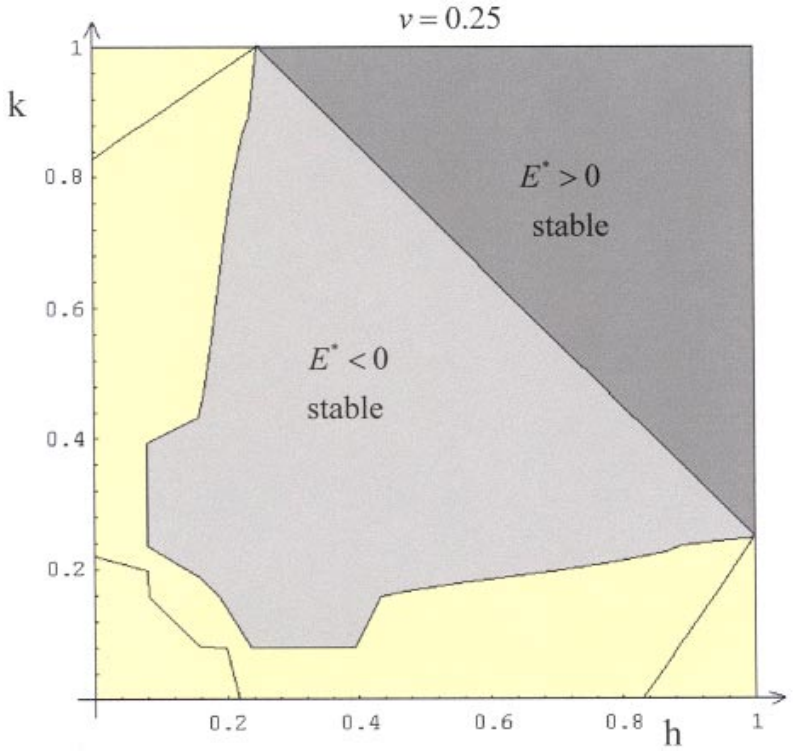

(c)

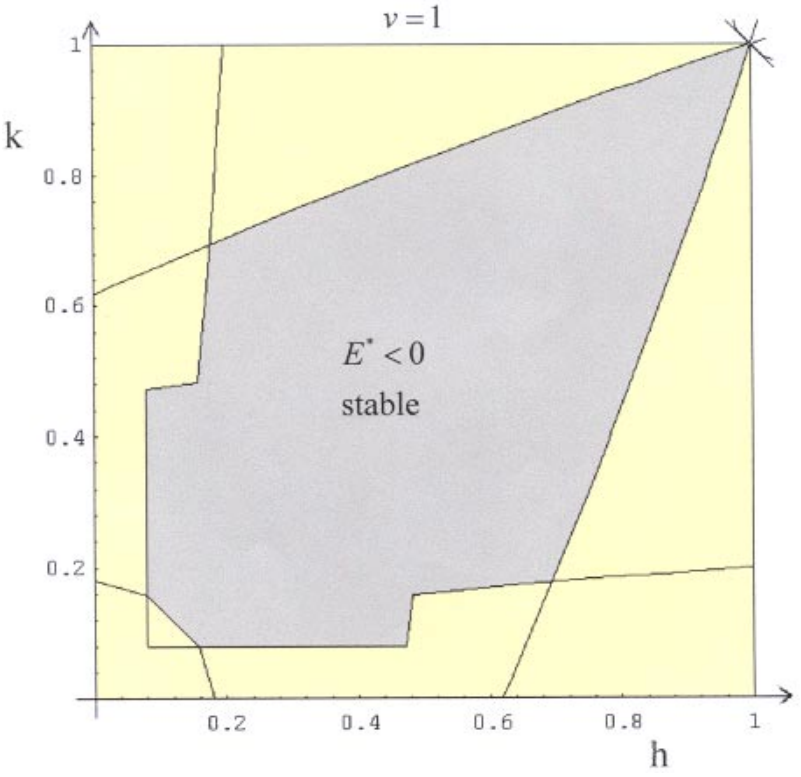

(d)

Fig. 1. (*Continued*)

In order to study the local stability of the Cournot equilibrium point the Samuelson conditions apply (see also [Agliari *et al.*, 2000]). These can be summarized as follows:

$$1 - M_2 + \mathrm{Det} > 0$$
$$1 - M_2 - \mathrm{Det} > 0$$
$$1 + M_2 - \mathrm{Det}^2 > 0$$

where Det is the determinant of the Jacobian matrix (15), i.e. $\mathrm{Det} = 2ABC$ and M_2 is the opposite of the sum of the principal minors of order two of (15), i.e. $M_2 = AB + BC + AC$.

It is easy to show that the second condition is always satisfied. By computer aid we further obtain that in the range of interest of parameters, the stability region is bounded by the curve $1 + M_2 - \mathrm{Det}^2 = 0$, (bifurcation curve), crossing which a subcritical Neimark–Hopf bifurcation appears, as we shall see in Sec. 6. Some stability regions in the parameter space (h, k), obtained at different values of v, are shown in Fig. 1. From that figure we can deduce that for high values of v, i.e. for low maximum obtainable price, the feasible trajectories are all converging to the fixed point [see Fig. 1(c)], in which the bifurcation curve does not cross the positivity region, dark-gray points, of E^*, whereas for lower values of v, also more complex dynamics in the feasible region can be obtained. In Figs. 1(a) and 1(b) the dark yellow points denote sets of parameters for which the fixed point is in the positive orthant of the space but it is unstable. Observe, as stated in Proposition 2, that when $v = 1$ [Fig. 1(d)] for each value of the parameter in the range of interest E^* has negative coordinates and no feasible trajectory exists.

4. Two Identical Producers

In this section we consider the particular case in which two producers have the maximum marginal cost, i.e. $h = 1$ in (7). This means that if the initial states of the outputs x and y, say x_0 and y_0, are equal, then the two players will "move" in the same way forever: $x_t = y_t$ for any $t \geq 0$. That is, their response to the market (though modified by the third oligopolist) is always the same. Certainly if their initial states are not equal, then their histories will be different, at least in a transient part, which may be very short, and it is possible (or highly probable, depending on the structure of the basins) that ultimately they will behave in the same way, or better, that their asymptotic behavior is similar.

Mathematically this comes from the fact that the plane Π^* of equation $y = x$ is trapping, i.e. mapped into itself, as the first two equations of the map T are equal. Thus all the points belonging to Π^* have trajectories trapped on that plane, which we shall call *invariant* for short (although it is strictly mapped into itself). It follows that the dynamics of points belonging to Π^* can be studied by use of a simpler map: the restriction of T to that invariant plane, which can be identified with a 2-D map. Let us denote by u the common value $x = y$, then the dynamics of T on Π^* can be reduced to the 2-D map, say T_u, given by:

$$T_u : \begin{cases} u' = \sqrt{u + z + v} - (u + z + v) \\ z' = \sqrt{\dfrac{2u + v}{k}} - (2u + v) \end{cases} \tag{16}$$

where a point $(u, z) \in \Pi^*$ identifies the point $(u, u, z) \in R^3$.

Let us now restrict our attention to the invariant plane in order to characterize the sets S and F. From the result obtained for the two-dimensional map T_u, we shall describe the dynamics of the whole map T in this particular case and we shall try to understand the generic case.

The domain of definition of the map (16) is

$$D_u = \left\{ (u, z) : u \geq -\frac{v}{2} \text{ and } u + z + v \geq 0 \right\} \tag{17}$$

In order to obtain the admissible and feasible regions, we consider the fixed point of T_u, which is given by

$$E_u^* = \begin{pmatrix} u^* \\ z^* \end{pmatrix} = \begin{pmatrix} \dfrac{k(1 + \sqrt{1 + v(k+2)}) - v(k+2)}{(k+2)^2} \\ \dfrac{(2-k)(1 + \sqrt{1 + v(k+2)}) - vk(k+2)}{(k+2)^2} \end{pmatrix}$$

Proposition 3. *For $k \in (0, 1]$ and $v \in [0, 1]$, the fixed point E_u^* of (16) belongs to the positive quadrant iff*

$$0 \leq v \leq k$$

and it is stable iff

$$v > \frac{k^3 - 5k^2 - 7k + 2 + (1-k)(2-k)\sqrt{k^2 - 4k + 1}}{18k^2}$$

and

$$0 < k < \frac{8 - 2\sqrt{13}}{3}$$

or

$$k \geq \frac{8 - 2\sqrt{13}}{3}.$$

At the bifurcation values, a Neimark–Hopf bifurcation takes place, i.e. complex eingenvalues cross the unit circle.

Proof. See Appendix B. ■

The stability region of E^* is shown in Fig. 2(a).

Let us complete the local stability analysis of the fixed point for T in the three-dimensional phase-space by computing the third eigenvalue of the 3-D Jacobian matrix J^* in (15), remembering that, in this particular situation, $A = B$. The third eigenvalue of J^* (always real) is given by

$$\lambda_3 = -A = \frac{2(1 + \sqrt{1 + v(2 + k)}) - (2 + k)}{2(1 + \sqrt{1 + v(2 + k)})}$$

It is simple to show that $0 < \lambda_3 < 1$, when v and k are in the range $[0, 1]$, thus λ_3 is always associated with a direction attracting towards the invariant plane, at least locally (near the fixed point), and the trajectories are locally on one side of that plane, i.e. they are not oscillating from one side to the other as it happens with a negative eigenvalue, which implies that the trajectories of points outside the invariant plane and near the fixed point cannot be symmetric with respect to the invariant plane.

In order to understand the structure of the basin of attraction of the attractors of the dynamical system and the structure of the admissible and feasible regions, a crucial role is played by the *Riemann foliation* induced by the map (see [Gumonwski & Mira, 1980a, 1980b; Mira *et al.*, 1996]), obtainable by the study of the critical line.

The map T_u in (16) is a noninvertible one: this means that while starting from some initial values for supplies, say (u_0, z_0), the iteration of (16) uniquely defines the trajectory $(u_t, z_t) = T_u^t(u_0, z_0)$, $t = 1, 2, \ldots$, the backward iteration of (16) may be not uniquely defined. In fact, a point (u, z) of the plane may have several rank-1 preimages. Calculating the preimages of a point $(u, z) \in R^2$ we obtain that

Proposition 4. *On the invariant plane the points* (u, z) *such that*

(a) $u > 1/4$ *or* $z > 1/4k$ *have no preimages, i.e. they belong to* Z_0;
(b) $u < 0$ *and* $z < 0$ *have one rank-1 preimage, i.e. they belong to* Z_1;
(c) $u < 0$ *and* $0 \leq z < 1/4k$ *or* $0 \leq u < 1/4$ *and* $z < 0$ *have two distinct rank-1 preimages, i.e. they belong to* Z_2;
(d) $0 \leq u < 1/4$ *and* $0 \leq z < 1/4k$ *have four distinct rank-1 preimages, i.e. they belong to* Z_4.

Thus, following the notation used in [Mira *et al.*, 1996], the map T_u is of the type $Z_1 - Z_2 - Z_4 - Z_0$, which means that the phase plane is subdivided into different regions Z_j $(j = 1, 2, 4)$ each point of which has j distinct rank-1 preimages and a region Z_0 of points without preimages.

The lines $u = 1/4$ and $z = 1/4k$, in the following $LC^{(1)}$ and $LC^{(k)}$ respectively, are the *Critical Lines*, loci of points with two merging preimages, and, as usual, separate the zones Z_0 and Z_j $(j = 2, 4)$. But in this case, due to the square root in the map, also the coordinate axes have this role, separating Z_4 from Z_2, and Z_2 from Z_1, see Fig. 2(b). But the points on the coordinate axes have distinct rank-1 preimages and so we cannot call them critical lines.

Geometrically, the action of a noninvertible map can be expressed by saying that it "folds and pleats" the plane, so that two or more distinct points are mapped into the same point, or, equivalently, that several inverses are defined which *unfold* the plane. The understanding of this mechanism is very important in our study, because we are interested in the topological structure of admissible and feasible regions, which are portions of the basin of attraction of the attracting sets of the map. And this strongly depends on contacts between critical sets and the boundary of the region. In fact, if a parameter variation causes a crossing between a basin boundary and a critical set (and in our case also the coordinate axes) which separates different region Z_k so that a portion H of a basin enters a region where a higher number of inverses is defined, then new components of the basin may suddenly appear, given by the new preimages of H. This is the basic mechanism which causes the creation of more and more complex structures of the admissible and feasible regions, as we shall see below.

For this reason, we end this section introducing some properties of the inverse transformation of T_u, useful in the following.

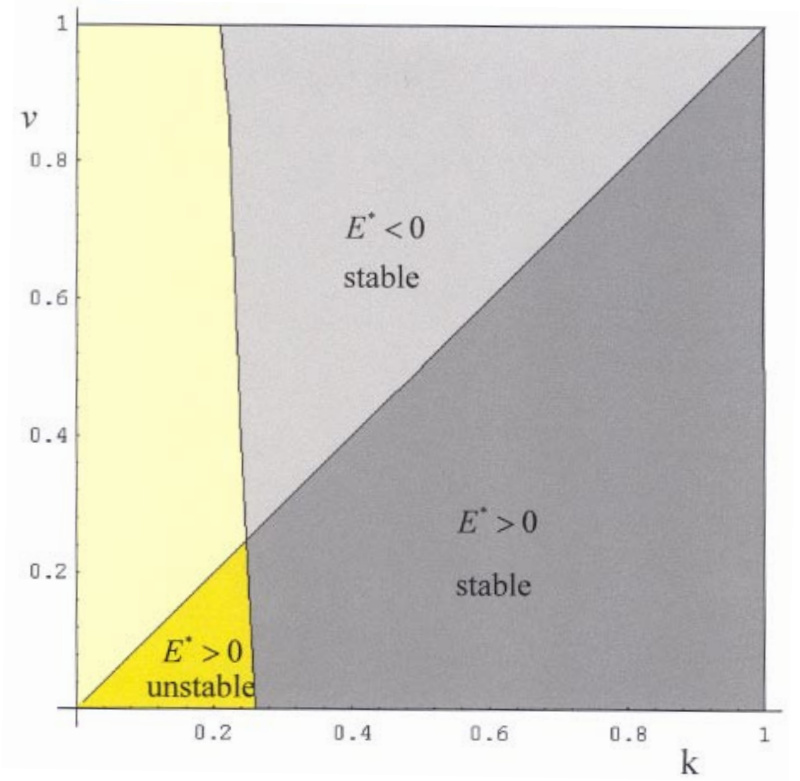

(a)

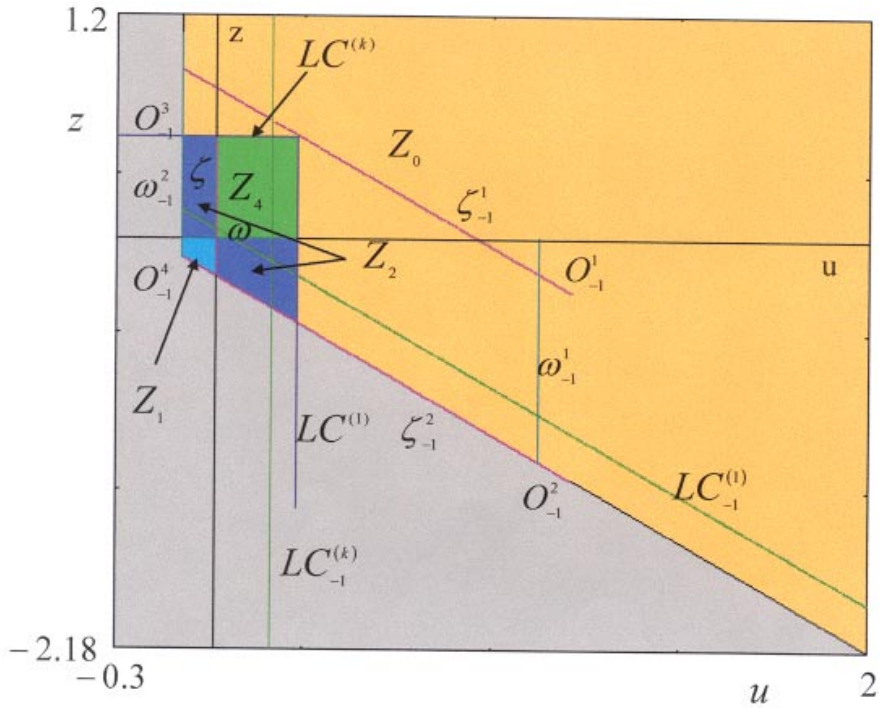

(b)

Fig. 2. (a) The stability region of E^* in the parameter space (k, v), obtained considering two producers with identical marginal costs, i.e. $h = 1$. (b) The domain of definition D_u of the map T_u, restriction of T to the trapping plane $x = y$ (Π^*), and its critical curves. The different colors denote the zones Z_0 (orange), Z_1 (light blue), Z_2 (blue) and Z_4 (green). The rank-1 preimages of the segments ζ and ω on the coordinates axes are also shown as well as the four rank-1 preimages of the point $O = (0, 0)$.

The preimages of the critical lines, loci of points of the merging preimages, are the *critical set of rank-0* and are given by the points for which the determinant of the Jacobian matrix vanishes. We obtain

$$LC_{-1}^{(1)} : \left\{ u + z = \frac{1}{4} - v \right\} \cap D_u$$

$$LC_{-1}^{(k)} : \left\{ u = \frac{1}{8k} - \frac{v}{2} \right\} \cap D_u$$

Let us define the half-lines

$$\begin{aligned} \omega &= \left\{ (u,\, 0) : u \le \frac{1}{4} \right\} \\ \zeta &= \left\{ (0,\, z) : z \le \frac{1}{4k} \right\} \end{aligned} \tag{18}$$

The preimages of ω and ζ are

$$\begin{aligned} &\omega_{-1}^{(1)} : \left\{ u = \frac{1}{2k} - \frac{v}{2} \right\} \cap D_u \text{ and} \\ &\omega_{-1}^{(2)} : \left\{ u = -\frac{v}{2} \right\} \cap D_u \\ &\zeta_{-1}^{(1)} : \{ z + u = 1 - v \} \cap D_u \text{ and} \\ &\zeta_{-1}^{(2)} : \{ z + u = -v \} \cap D_u \end{aligned} \tag{19}$$

From (19) it is easy to obtain the four preimages of the origin, the points of intersection of these segments, as shown in Fig. 2(b), which are

$$O_{-1}^{(1)} = \left(\frac{1}{2k} - \frac{v}{2},\, 1 - \frac{1}{2k} - \frac{v}{2} \right)$$

$$O_{-1}^{(2)} = \left(\frac{1}{2k} - \frac{v}{2},\, -\frac{1}{2k} - \frac{v}{2} \right)$$

$$O_{-1}^{(3)} = \left(-\frac{v}{2},\, 1 - \frac{v}{2} \right) \quad O_{-1}^{(4)} = \left(-\frac{v}{2},\, -\frac{v}{2} \right)$$

Another important property of the map T_u is that the rank-1 preimages of segments belonging to a line $u = \text{const}$, when they exist, are located on a straight line parallel to $u + z = 0$ and those of segments belonging to a line $z = \text{const}$, when they exist, are located on a straight line of type $u = \text{const}$ [see Fig. 2(b)].

5. Global Bifurcations in the Feasible Regions F_u and F

In this section, we shall study the geometrical structure of the admissible and, in particular, feasible regions of the model (16) as the marginal cost k of the third producer is varied in the stability region of the fixed point E^*. In order to help the understanding of the different situations we deal with, the section is organized in three subsections: the first one is devoted to the description of the admissible region S_u, obtained by the preimages of the boundary of the definition set D_u. The second one describes the feasible region F_u as a convex set which can have different shapes, depending on the rank of the preimages of the coordinate axes to be considered. In the last subsection the topological structure of F_u is more complex, caused by contact bifurcation between its frontier and the critical sets. In any subsection the corresponding regions S and F, related to the three-dimensional map T, are described. Although in our examples we consider $v = 0.2$, analogous results can be obtained for low values of v ($v \le 0.5$), i.e. for relatively high maximum price obtainable, as should be.

5.1. *Admissible regions*

The starting situation we consider is given in Fig. 3(a), in which $k = 0.46$. In that figure we can observe the set of feasible points F_u (yellow points) and the admissible but unfeasible points (the red ones) on the invariant plane Π^*. Obviously the set of all non-gray points is the section S_u of S on Π^* and F_u is the section of F, always on the same plane.

With this choice of parameters, the Cournot equilibrium point is the unique attractor of the map T_u and its basin of attraction ($\mathcal{B}_u(E^*)$) is the whole admissible region S_u. We observe that both $\mathcal{B}_u(E^*)$ and F_u are connected sets. Now we show how the boundary of S_u depends on the *Riemann foliation* of the map.

Consider the set $\mathcal{B}_u(E^*)$. Its frontier can be constructed considering the set of definition D_u in (17) of the map and, in particular, the four segments

(i) VD on $u = -(v/2)$, where V is the vertex of D_u, i.e. $V = (-(v/2),\, -(v/2))$ and D also belongs to the u-axis, i.e. $D = (-(v/2),\, 0)$. Its points have only one rank-1 preimage;

(ii) DA on $u = -(v/2)$, where A also belongs to $LC^{(k)}$, i.e. $A = (-(v/2),\, 1/4k)$. Its points have two rank-1 preimages;

(iii) VC on $u + z = -v$, where C also belongs to the z-axis, i.e. $C = (0,\, -v)$. Its points have only one rank-1 preimage;

(iv) CB on $u + z = -v$, where B also belongs to $LC^{(1)}$, i.e. $B = (1/4, -v - (1/4))$. Its points have two rank-1 preimages.

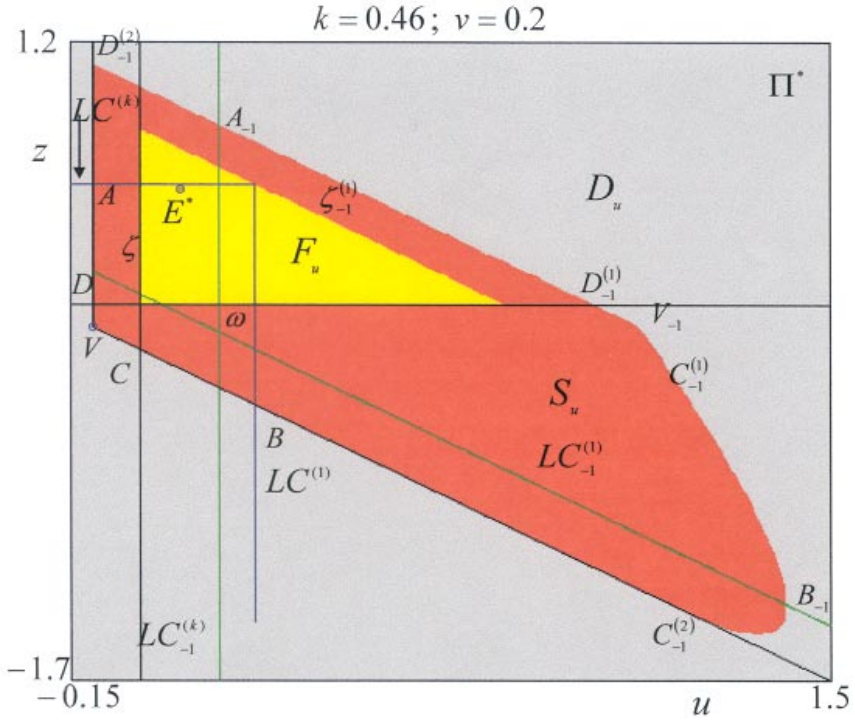

(a)

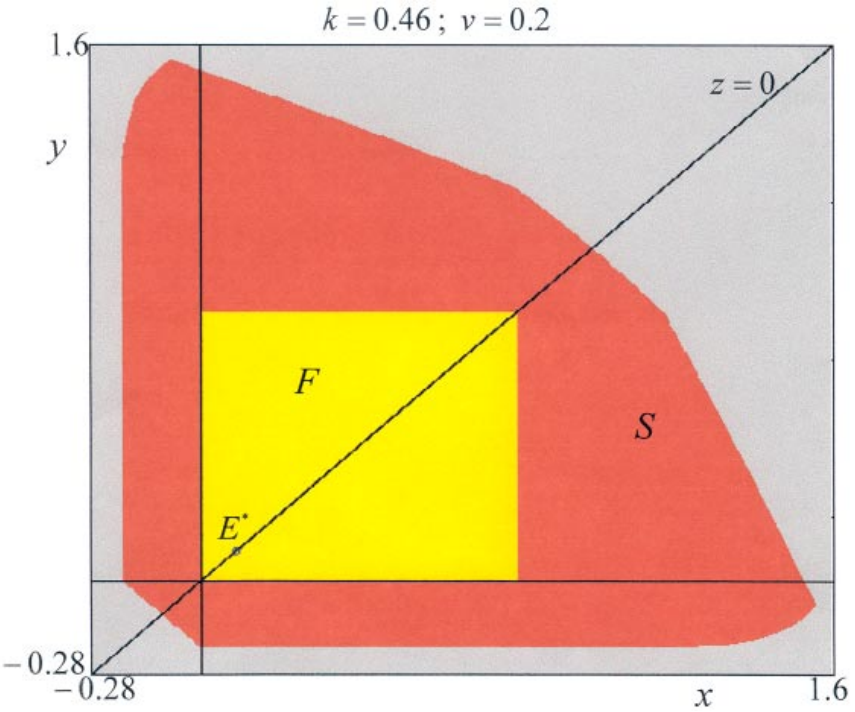

(b)

Fig. 3. (a) The basin of attraction of the stable fixed point E^* on the plane Π^*. The yellow points denote the set of feasible trajectories F_u, the red ones the set of admissible but unfeasible trajectories. The union of yellow and red sets give the admissible set S_u, whose points all converge to E^*. The gray points in D_u represent the nonadmissible trajectories. The boundary of S_u is obtained considering the rank-1 preimages of the segments AV and VB. The upper frontier of the feasible set F_u is given by the rank-1 preimages of the segment ζ. (b) The plane section with the plane $z = 0$ of the admissible $(F \cup S)$ and feasible (F) sets for the three-dimensional map.

The preimages of VD and DA belong to a straight line parallel to $u + z = -v$, as observed in Sec. 4: they give the upper boundary of S_u. In particular, the preimages of DA are the two segments located on opposite sides of $LC_{-1}^{(k)}$, with a common extremum A_{-1}, corresponding to the two merging preimages of A, the others extrema are given respectively by $D_{-1}^{(1)}$ and $D_{-1}^{(2)}$, the two preimages of D. The last part of the upper frontier is given by the preimages of VD, i.e. the segment between $D_{-1}^{(1)}$ and V_{-1}, the preimage of V. The curve which closes $\mathcal{B}_u(E^*)$ is given by the preimages of VC and CB: more precisely the preimages of CB are the two arcs located on opposite sides of $LC_{-1}^{(1)}$, with a common extremum B_{-1}, corresponding to the two merging preimages of B, the others given respectively by $C_{-1}^{(1)}$ and $C_{-1}^{(2)}$, the two preimages of C, and the preimages of VC are located in the upper part of the curve, between V_{-1} and $C_{-1}^{(1)}$. Because all these preimages belong to Z_0, there are no preimages of rank-k ($k > 1$) of VD, DA, VC and CB, and the construction of the boundary of $\mathcal{B}_u(E^*)$ is completed by adding the appropriate portions of the frontier of D_u.

Now considering the basin $\mathcal{B}(E^*)$ of the fixed point in three-dimensional space R^3, we have that it is a simply connected volume, whose boundary we conjecture is determined by the rank-1 preimages of the portion of planes defining the boundary of the domain of definition of the map, and not belonging to the region Z_0. That is, the rank-1 preimages of the portions on the planes $y+z+v = 0$, $x+z+v = 0$, $x + y + v = 0$:

$$\partial\mathcal{B}(E^*) = \partial S = \mu \cup T^{-1}(\mu)\,, \quad \mu = \partial D \backslash Z_0$$

In order to confirm this fact we can consider the sections of S with planes $z = \overline{z}$, which all appear as connected sets, if $\overline{z}$ varies in a bounded interval: in Fig. 3(b) the section $z = 0$ is shown.

Evidently, when some of the preimages of increased rank of μ appear, due to a contact bifurcation of the frontier of the regions with the critical surfaces, they cause a qualitative change in the structures of S_u and S. In the following we do not proceed with the study of the admissible regions, because the different situations we find are qualitatively the same as in [Agliari *et al.*, 2000].

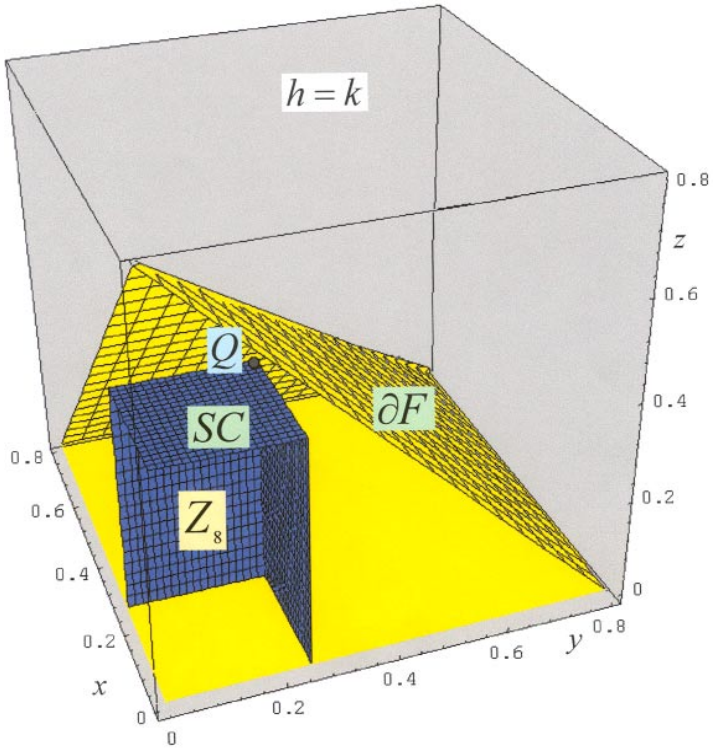

Fig. 4. The pyramidal shape of the feasible set F (in yellow), bounded by the coordinate planes and the rank-1 preimages of $x = 0$ and $y = 0$ (the two transverse planes denoted by ∂F). The critical set SC (in blue) of the map T, located below ∂F, is also shown. Only the points belonging to the convex set bounded by SC have preimages, eight if feasible.

5.2. *Connected feasible regions*

More interesting is the study of the feasible region, the only meaningful one in the economic application. As before, we start by describing F_u and try to understand the structure of F in the whole space. In order to obtain the boundary of F_u, we now have to consider the coordinate axes, which separate the points with positive coordinates from the others. In Fig. 3(a) we observe that the major part of the rank-1 preimages of both the segments ω and ζ, given by (19), are out of the positive quadrant of Π^* (in the following Π^*_+). Thus, the feasible region has a triangular shape, bounded by portions of the coordinate axes and by the portion of $\zeta^{(1)}_{-1}$ belonging to Π^*_+. From an economic point of view, this means that the producer with lower marginal cost (equals k), can gain by producing a quantity $z \le 1 - v$ (positioning the market on $\zeta^{(1)}_{-1}$) so as to throw the two identical players out of the market, because they do not obtain any profits. The competitors do not have this possibility, because they have a too high marginal cost: in order to stay in the market they have to produce a total quantity $x + y \le 1 - v$, and if $x + y = 1 - v$, then the profit of the competitor is zero. But they do not gain, making no profit either. Moreover the third producer can produce an arbitrarily low quantity in order to obtain a price near the maximum price obtainable. This is also true if the two producers do not behave in an identical way (out of the invariant plane): in fact the feasible region F in R^3 has a square-based pyramidal shape, shown in Fig. 4, contained in the cube $[0,\, 1-v] \times [0,\, 1-v] \times [0,\, 1-v]$. The boundary of F is given by the rank-1 preimages of the coordinate planes $x = 0$ and $y = 0$.

In Fig. 4 the critical set of the map T is also illustrated, bounding a Z_8 region with the coordinate planes. In fact, as stated in Proposition 5 in Sec. 7, the map T is also noninvertible and is defined in the space regions of points (*zones*) with different numbers of rank-1 preimages. In particular, in the positive orthant of the space (R^3_+) only the points belonging to the convex parallelepiped bounded by the critical surfaces (which are planes) have preimages, and exactly eight, of which only four belong to the invariant plane Π^*. Observe that the preimages of the planes $x = 0$ and $y = 0$ belong to Z_0, then they completely define the region F.

This situation persists until the marginal cost k is sufficiently small. In fact, we can observe in Fig. 5(a) where k is increased, that the triangular shape of F_u is lost: the feasible region is always a connected set, but now it has a trapezoidal shape. How can we explain this change in the structure of F_u? In order to give an answer to this question, let us return to the previous analysis. We have said that both the segments ω and ζ have four preimages, but only $\zeta^{(1)}_{-1}$ was in Π^*_+. Observe now that $\omega^{(2)}_{-1}$ and $\zeta^{(2)}_{-1}$ are in $\Pi^* \setminus \Pi^*_+$ for each value of k (and v), because they are the frontier of S_u, but a portion of $\omega^{(1)}_{-1}$ can enter Π^*_+: when

$$k \ge \frac{1}{2 - v}$$

i.e. the point $O^{(1)}_{-1}$, rank-1 preimage of O, belongs to Π^*_+. This is the case of Fig. 5(a): now the boundary of F_u is given by portions of the coordinate axes and by part of $\zeta^{(1)}_{-1}$ and $\omega^{(1)}_{-1}$. Looking at the section shown in Fig. 5(b), we can observe that in the whole space R^3, the pyramid representing the feasible region F is now truncated short of the vertex $(1 - v,\, 1 - v,\, 0)$ by a plane parallel to $z = 0$ and orthogonal to the plane $x = y$, i.e. $x + y = (1/k) - v$. So, also if the two producers with the highest marginal cost, behave differently, they have the possibility to win the market, until $z \le 1 - (1/2k) - (v/2)$.

For higher values of v, until $v \le 0.5$, the structure of the feasible regions remains the same, also when k increases towards 1.

5.3. *Contact bifurcations in F*

Let us return to the case $k < 1/(2 - v)$. In this section we shall study the effect on F_u (and F) of the contact bifurcation, arising when the point $Q = (1/4,\, 1/4k)$ on Π^*, i.e. $Q = LC^{(1)} \cap LC^{(k)}$, belongs to the upper boundary of F_u. This happens when k becomes equal to

$$k_{cb} = \frac{1}{3 - 4v}$$

The vertex Q has four preimages merging in $Q_{-1} = ((1/8k) - (v/2),\, (1/4) - (1/8k) - (v/2))$, the point in which $LC^{(1)}_{-1}$ and $LC^{(k)}_{-1}$ intersect. Observe that the z-coordinate of Q_{-1} is negative in the range of values at which we are now interested ($v \le 0.5$ and $k \le 1/(3-4v)$) and this means that such a point belongs to a region of admissible but unfeasible trajectories. For that reason, when we decrease a bit k from k_{cb} [Fig. 6(a)] we do not see (as expected)

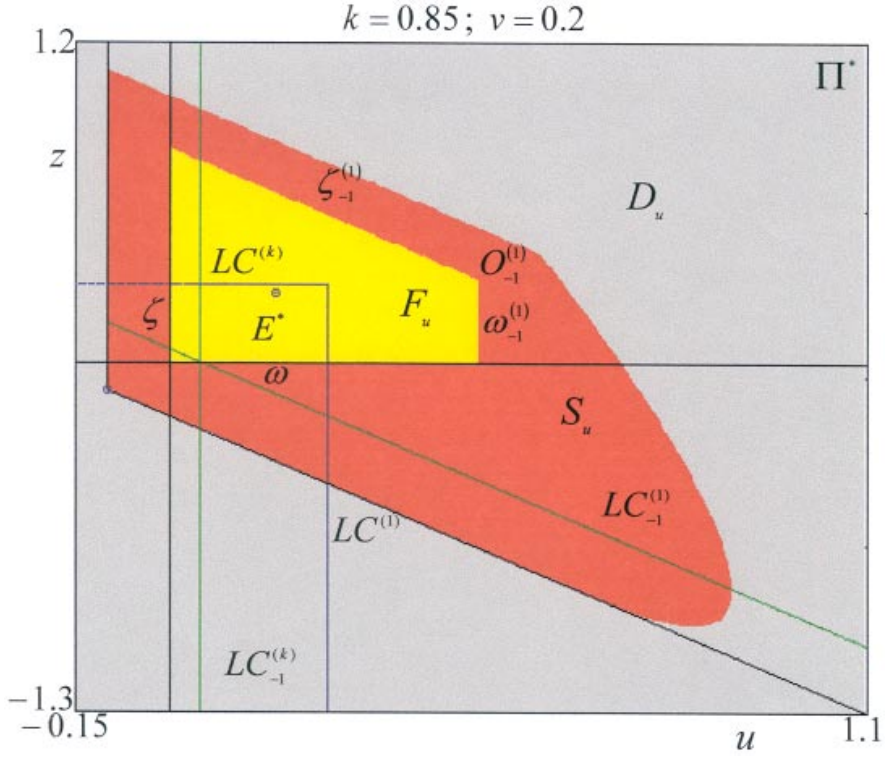

(a)

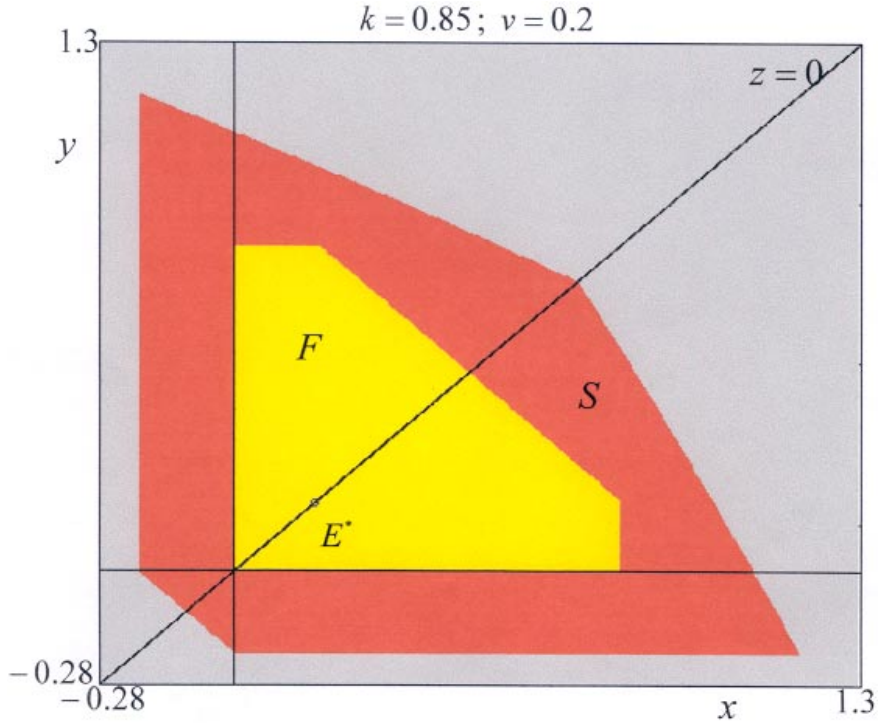

(b)

Fig. 5. (a) The feasible set F_u on the plane Π^* is a convex set, with a trapezoidal shape. This is due to the rank-1 preimages of the segment ω that, for high values of k, enter the feasible region. (b) The plane section with the plane $z = 0$ of the basins of attraction of E^*. The yellow points are the basis of the truncated pyramid representing the feasible region F.

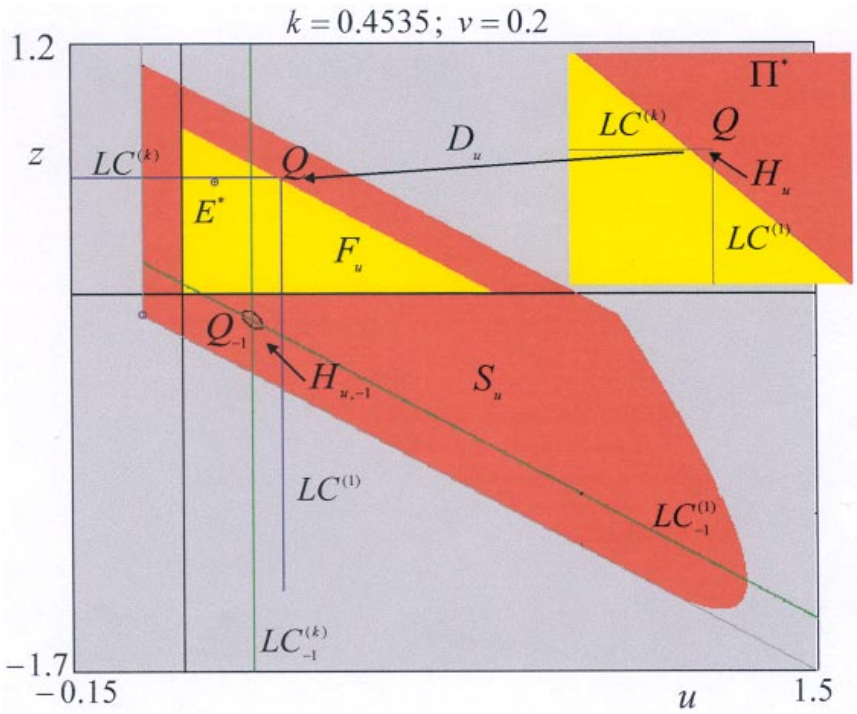

(a)

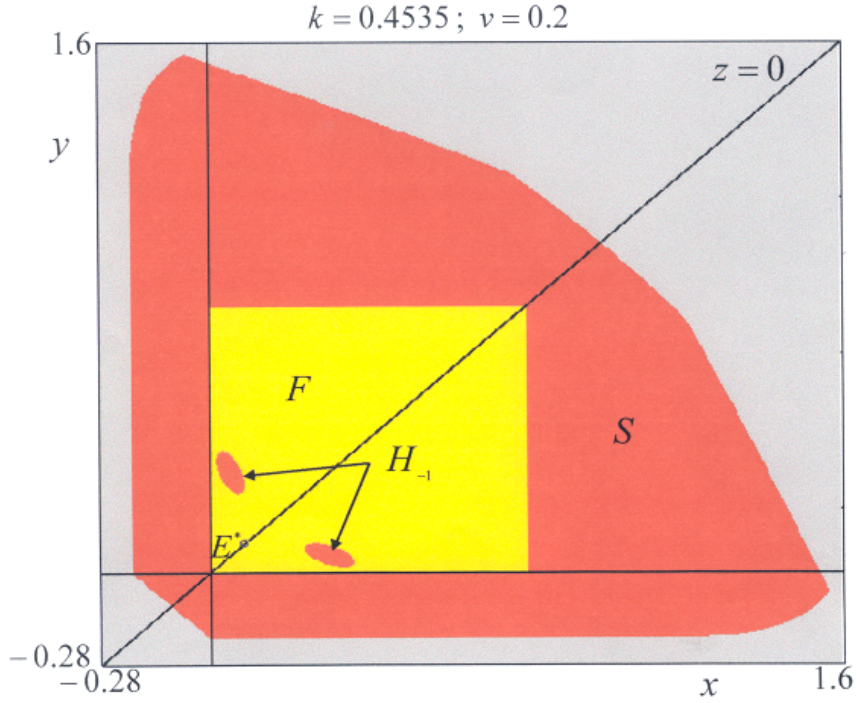

(b)

Fig. 6. (a) After the contact bifurcation value, occurring when the vertex $Q = LC^{(1)} \cap LC^{(b)}$ belongs to the upper boundary of F_u, the unfeasible points in the set H_u enter into Z_4. The feasible region F_u on the invariant plane is always a convex set, because the hole $H_{u,-1}$ of the rank-1 preimages of H_u, located around the point Q_{-1} (the four merging preimages of Q) does not intersect the "old" feasible region. (b) The effects of the contact bifurcation are visible on the plane $z = 0$: the two red balls (unfeasible points) inside the yellow square are the sections of the rank-1 preimages of an unfeasible volume H containing the point Q.

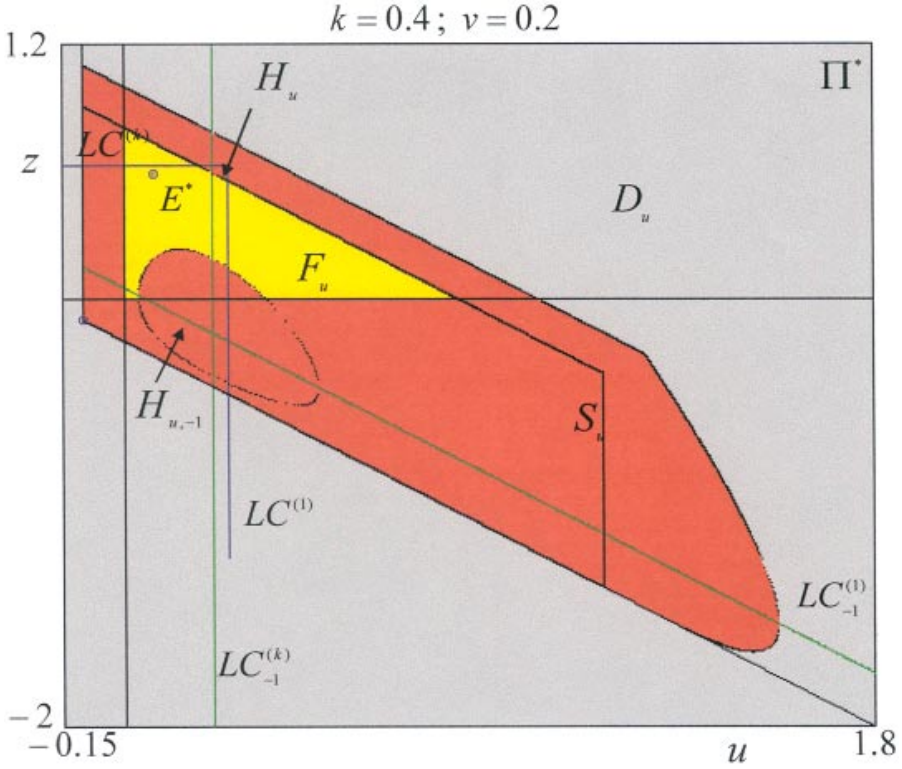

(a)

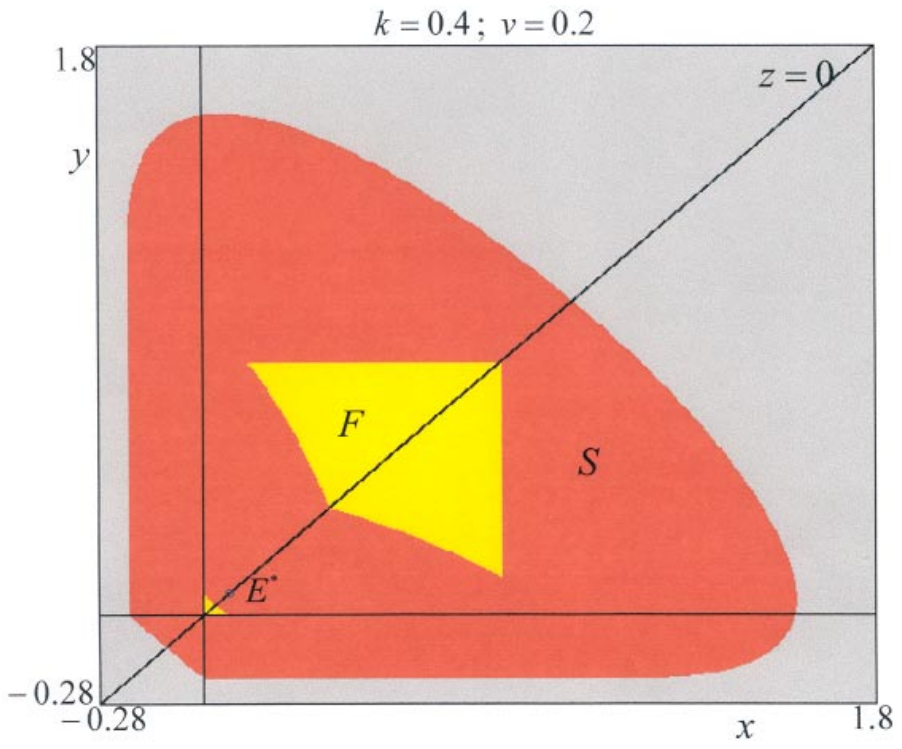

(b)

Fig. 7. (a) As k is further decreased, the hole $H_{u,-1}$ becomes bigger and bigger and gets into contact with the region F_u, which becomes a connected, not convex set. (b) Plane section of the region F with the plane $z = 0$. F is always a connected, not convex set, the two yellow pieces which appear in the figure joining itself near $z = 0.5$.

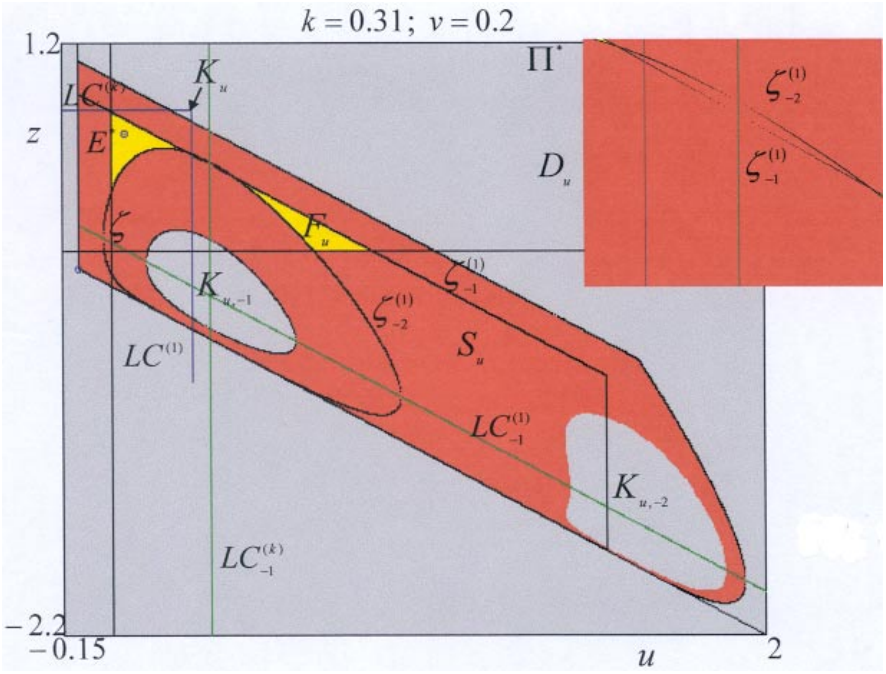

(a)

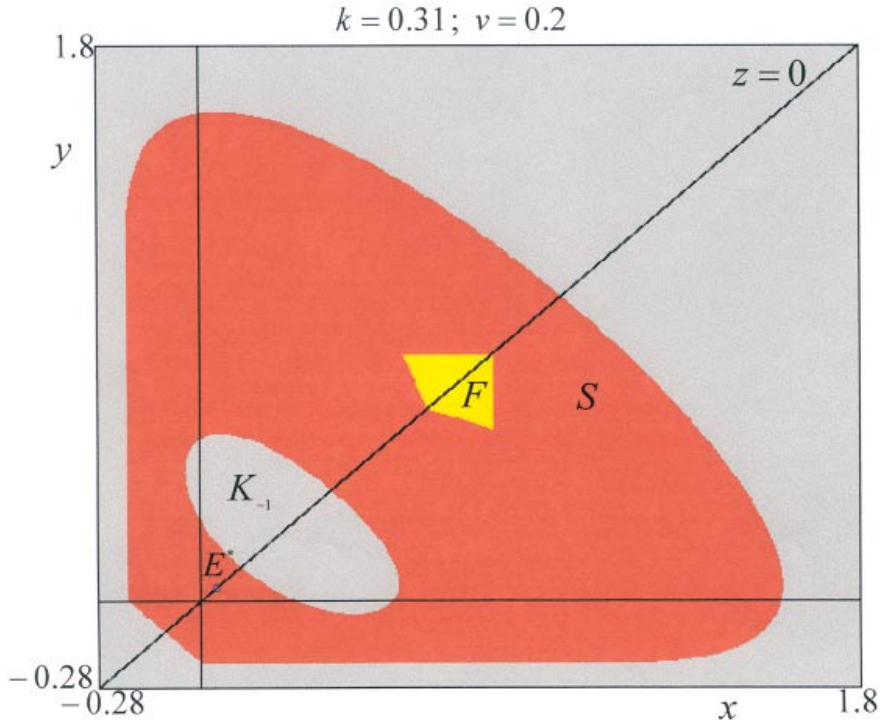

(b)

Fig. 8. (a) For small k, the region F_u is a disconnected set, due to the contact between its upper boundary and the boundary of $H_{u,-1}$ (see enlargement). Moreover, a global bifurcation in the admissible region occurs, due to the contact of Q with the upper boundary of S_u, leading to a multiply connected set. K_u is the set of nonadmissible points entering the Z_4 region; the holes $K_{u,-1}$ and $K_{u,-2}$ of nonadmissible points are the preimages of K_u of rank-1 and rank-2, respectively. (b) Plane section of F and S with the plane $z = 0$. In this case, the feasible region F is formed by two separated volumes, only one of them intersects the plane $z = 0$. The gray hole K_{-1} inside the set S denotes the rank-1 preimages of the volume K of which K_u is the section on Π^*.

a qualitative change in the set F_u. In fact, a set H_u of admissible but unfeasible trajectories is in Z_4, but its preimages, the hole $H_{u,-1}$ around Q_{-1}, do not have any contact with F_u, leaving its shape unchanged. This occurs on the invariant plane Π^*, but if we look at the sections of F on plane $z = \overline{z}$ [Fig. 6(b) shows the section $z = 0$] we note that the feasible region in the whole space is always a connected set (but not a convex one) given by the "old" pyramid, where we have to remove two sorts of balls, put on the face $z = 0$. These unfeasible points are the (four) preimages of the volume H, containing the point $(1/4, 1/4, 1/4k)$, located outside of Π^*, of which H_u is the section on the invariant plane.

If k is further decreased, the hole $H_{u,-1}$ (and obviously H_{-1}) becomes bigger and bigger, and gets in contact with the region F_u, so that this last one assumes a more complex structure: a connected nonconvex set or even a disconnected set [Figs. 7(a) and 8(a)], due to different contact bifurcations of the same type. In any case, the shape of F_u can be obtained by the preimages of increased rank of the segment ζ. In particular, the disconnected shape of F_u is due to a new contact between $\zeta_{-1}^{(1)}$ and the boundary of $H_{u,-1}$ [see the enlargement in Fig. 8(a)]. Looking at the sections, we observe that F can also assume a complex structure: in the first case, on the plane $z = 0$, shown in Fig. 7(b), two pieces, which join itself near $z = 0.5$, in the second case, F is disconnected, being formed by two separate volumes, of which only one intersects the plane $z = 0$, as shown in Fig. 8(b).

In Fig. 8(a), we can also see that a global bifurcation for the admissible set S_u has taken place: the set S_u now is a multiply connected set. This qualitative change of the admissible region is due to a contact bifurcation between its frontier and the critical set which arises when the point Q belongs to the upper boundary of S_u. After this contact a region K_u of nonadmissible points is in Z_4 and its preimages give the gray holes inside the admissible region. In the example we consider, the rank-1 preimages of K_u define the hole around Q_{-1} and the other one is given by the rank-2 preimages of K_u. Obviously the structure of the volume S is also modified by this contact bifurcation, as we can see in Fig. 8(b).

The ones described above are some of the feasible region structures that accompany the maps T_u and T, for low values of v. If we consider a higher value of v (for example $v > 0.5$), different structures are possible, but the bifurcations, causing the qualitative changes of F_u or F, are similar to those just described. In the next section we study the dynamics associated with the map T_u and we will also find an important qualitative change in the structure of the feasible region due to a global bifurcation of a different type (bifurcation of "saddle-node type").

6. Complex Dynamics of the Map T_u

In this section we are interested in the dynamics of the map T_u in (16), when the marginal cost k and the parameter v are so chosen that the bifurcation curve in Fig. 2(a) is crossed. In particular, we shall study what happens when the crossing is from the dark gray region (the equilibrium point is stable and feasible) to the yellow one (E^* is feasible but unstable). We know, from Proposition 3, that the loss of stability of E^* is due to a Neimark–Hopf bifurcation. We shall see that, as in the subcase studied in [Agliari *et al.*, 2000], this bifurcation is of *subcritical type*, i.e. a repelling closed invariant curve exists "around" the stable fixed point, decreasing in size and merging with the fixed point at the bifurcation value (k_{bif}^v) and so "transforming" it into an unstable one. Before starting, it is important to note that only for low values of v, E^* can become unstable and feasible: only $v \leq 0.25$ has to be considered (see Fig. 1). For that reason, we consider small values of v, in order to obtain more interesting situations.

We start considering $v = 0.01$ and then a value of k close to $k_{\text{bif}}^{0.01}$, at which the Neimark–Hopf bifurcation takes place. For $k = 0.2627$ the fixed point E^* is stable, its basin of attraction, $\mathcal{B}(E^*)$, is a multiply connected set and all the points of the feasible region F_u have trajectories converging to E^* [see Fig. 9(a)]. The set F_u is disconnected, because a sequence of bifurcations like the ones described in the previous section occurred; anyway, the boundary of F_u can be obtained by the coordinate axes and their preimages. If we consider somewhat smaller k, we can observe that in F_u there are points not converging to E^*. This is however still attracting but $\mathcal{B}(E^*)$ has a very different shape. In fact, as we see in Fig. 9(b), now we have the coexistence of two attractors: the fixed point E^* and a closed invariant attractive curve Γ_s. The appearance of Γ_s is due to a global bifurcation (called *saddle-node type* bifurcation), occurring at a value of k, say $k_{\text{sn}}^{0.01}$, not easily detectable, but smaller than $k_{\text{bif}}^{0.01}$: this

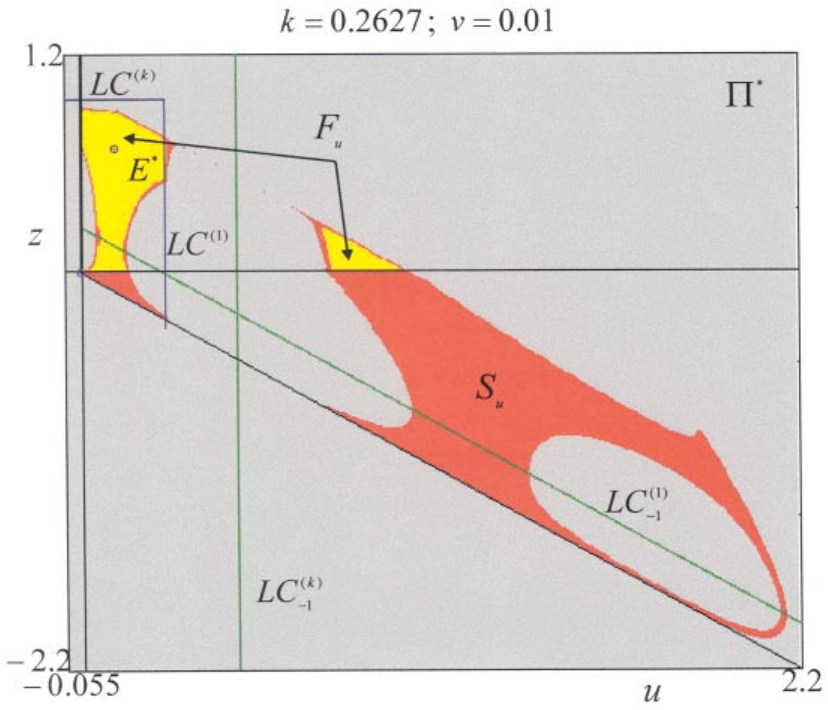

(a)

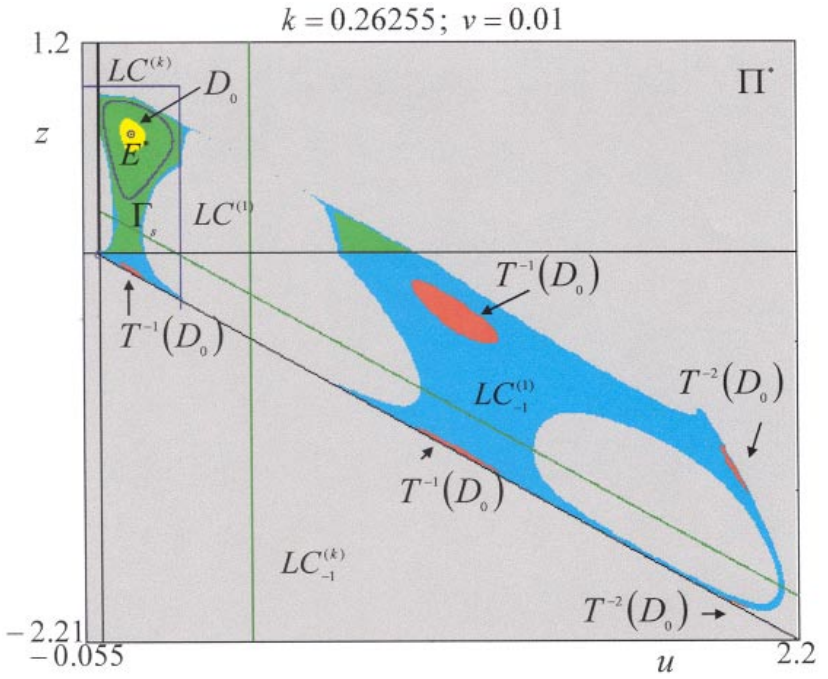

(b)

Fig. 9. Complex dynamics at $v = 0.01$. (a) The basin of attraction of the attracting fixed point E^* on the invariant plane. The feasible region F_u is a disconnected set. (b) A global bifurcation occurred giving rise to the birth of two closed invariant curves, one attracting Γ_s and one repelling Γ_u. The fixed point is still attractive. The basin of E^* is a disconnected set given by the immediate basin D_0 (yellow points), whose boundary is the repelling curve, and its preimages of ranks 1 and 2 (red points). Only the points belonging to D_0 are feasible. The basin of attraction of Γ_s is given by the green and light blue points, the green ones being feasible. (c) Plane section with the plane $z = 0.7$ of the basins of attraction of E^* and of Γ_s, separated by the stable manifold of the invariant curve Γ_u. (d) After the subcritical Neimark–Hopf bifurcation, the fixed point is unstable and the only surviving attractor is Γ_s. All the feasible points (in green) belong to the basin of attraction of Γ_s. (e) As k is further decreased, the curve Γ_s has a contact with the z-axis, after which no feasible trajectory exists.

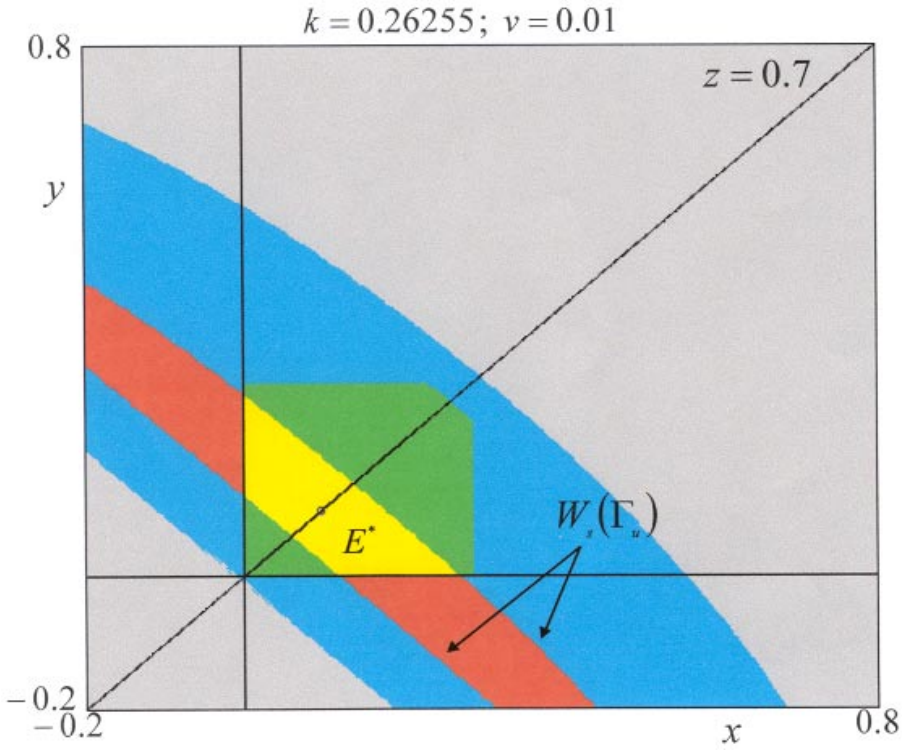

(c)

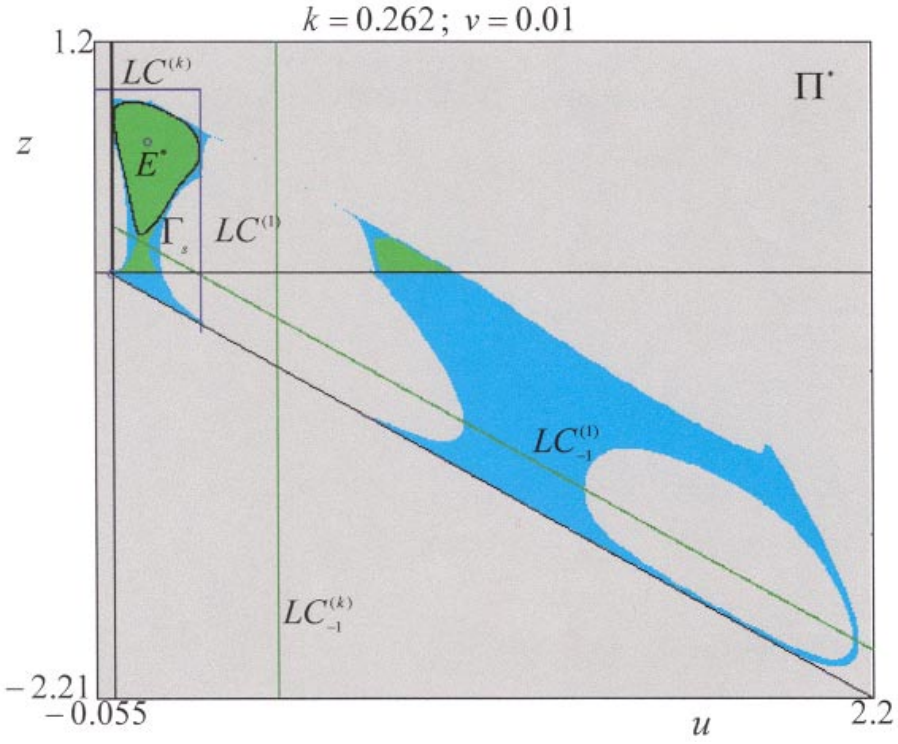

(d)

Fig. 9. (*Continued*)

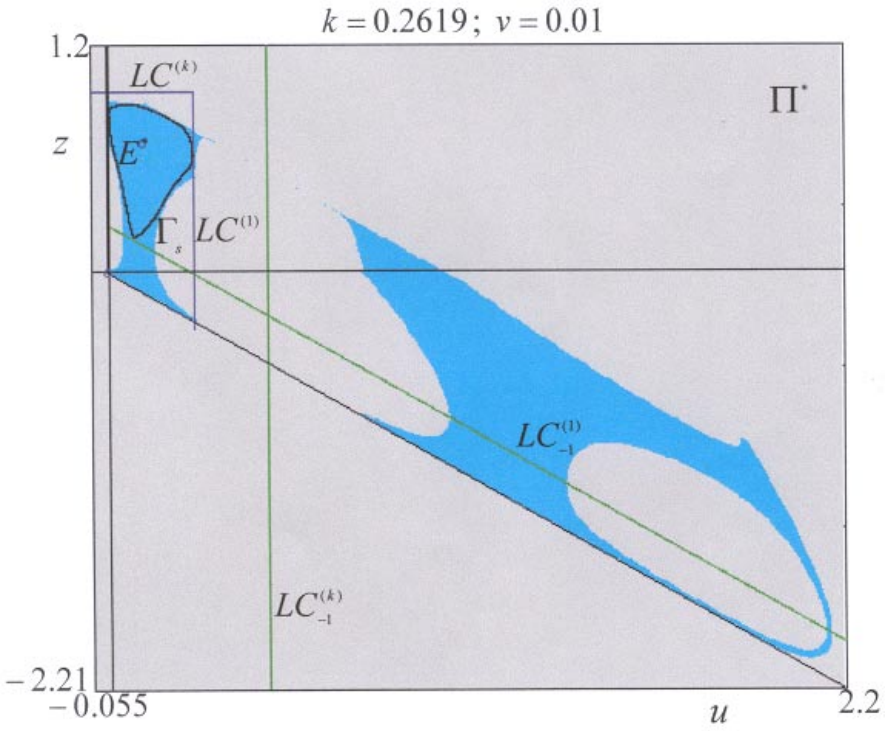

(e)

Fig. 9. (*Continued*)

bifurcation gives rise to two invariant closed curves, one attracting Γ_s, and one repelling Γ_u, belonging to the invariant plane. Both Γ_s and Γ_u are in the feasible region F_u, Γ_u being the boundary of the immediate basin of attraction D_0 of E^* (i.e. the largest connected component of $\mathcal{B}(E^*)$). In F_u we have points (the green ones) converging to Γ_s and points (the yellow ones) converging to E^*: in particular the largest portions of the feasible trajectories are in $\mathcal{B}(\Gamma_s)$. The set $F_u \cap \mathcal{B}(E^*)$ is the immediate basin of E^*, with boundary Γ_u, the whole stable set on the invariant plane of Γ_u being the boundaries of the preimages of D_0 (six sets, one in yellow and five in red) which with D_0 constitute the disconnected set $\mathcal{B}(E^*)$. Some preimages of D_0 are located outside the invariant plane Π^*, so that for the whole map T the feasible points in the basin of E^* consists of two volumes of the space, as the sets of feasible points converging to Γ_s. In Fig. 9(c) the section $z = 0.7$ (near the fixed point) of the admissible region is shown. As the parameter k is further decreased, the two closed curves, Γ_u and Γ_s, move away from each other, and Γ_u decreases in size until, at the bifurcation value $k_{\text{bif}}^{0.01}$, it shrinks to the fixed point and it disappears, leaving E^* unstable: this is the Neimark–Hopf bifurcation of subcritical type. For $k < k_{\text{bif}}^{0.01}$, the only surviving attractor is Γ_s and the feasible trajectories belong to $\mathcal{B}(\Gamma_s)$. In Fig. 9(d) we observe that Γ_s is close to approaching the boundary of the feasible region, and in fact, for a lower of value of k, after contact with the z-axis, the feasible region F_u disappears [Fig. 9(e)]: in this case the generic admissible trajectory is unfeasible.

The saddle-node global bifurcation and the subcritical Neimark–Hopf bifurcation can be found also for greater values of v, but their effect on the region of feasible trajectories is not the same.

For example, at $v = 0.06$, the closed attractive curve Γ_s, born at $k = k_{\text{sn}}^{0.06}$, is not contained in the region F_u, so we do not have feasible trajectories converging to it. In Fig. 10(a), we see that the feasible region is composed of two separate components, both subsets of $\mathcal{B}(E^*)$, the immediate basin D_0 and a portion of $T^{-1}(D_0)$: The frontier of F_u is now given by the closed repelling curve Γ_u and a portion of its stable set belonging to F_u. For F the same argument may be applied. Obviously, after the Neimark–Hopf bifurcation, i.e. at

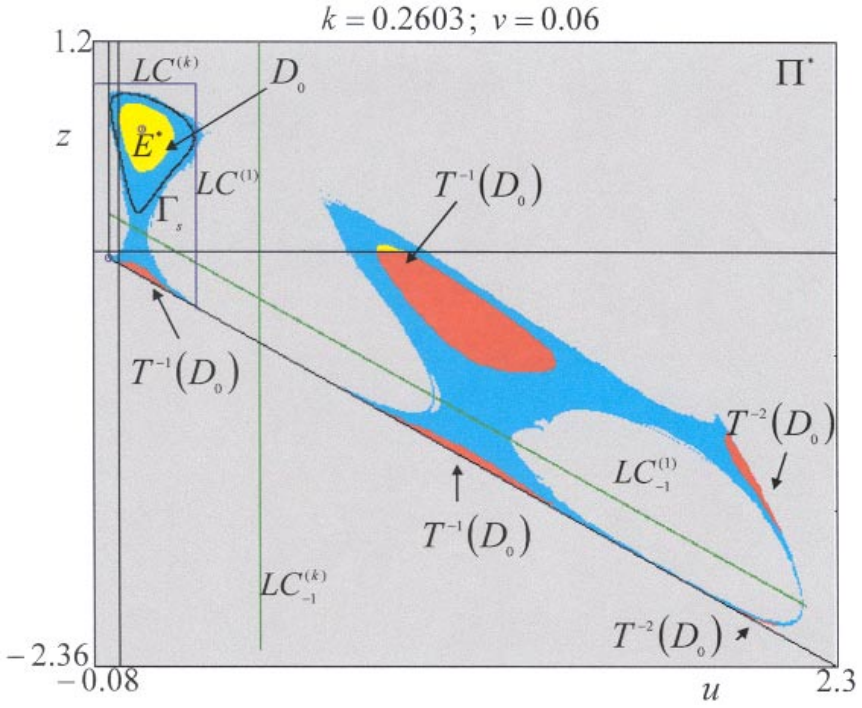

(a)

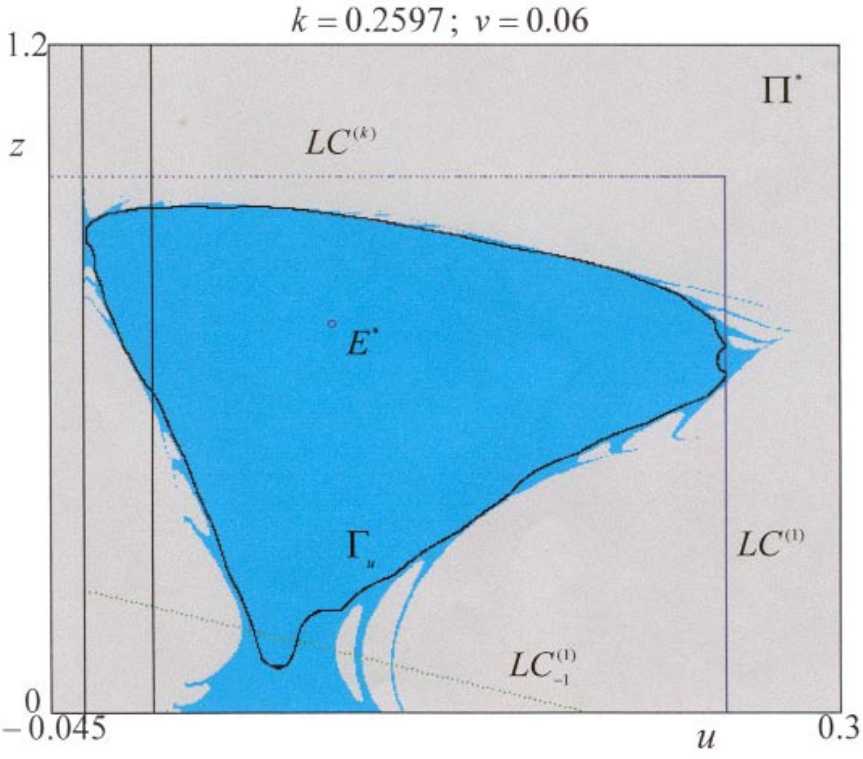

(b)

Fig. 10. Complex dynamics at $v = 0.06$. (a) The attracting curve Γ_s coexists with the attracting fixed point, but it crosses the z-axis. No feasible trajectory converging to Γ_s exists. The feasible region now is a very small disconnected set, given by the immediate basin D_0 of E^* and a small portion of the rank-1 preimages of D_0. (b) Enlargement of the set of bounded trajectories. After the Neimark–Hopf bifurcation, no feasible trajectory exists. In this example, Γ_s crosses $LC^{(1)}_{-1}$, this implies the folding of Γ_s on $LC^{(1)}$ and the appearance of smooth oscillations on its shape.

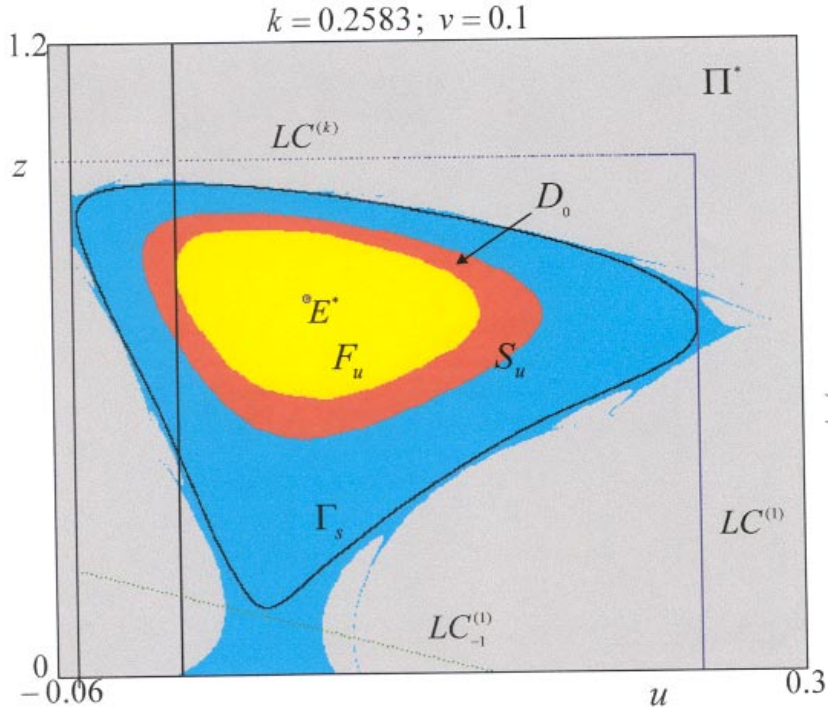

(a)

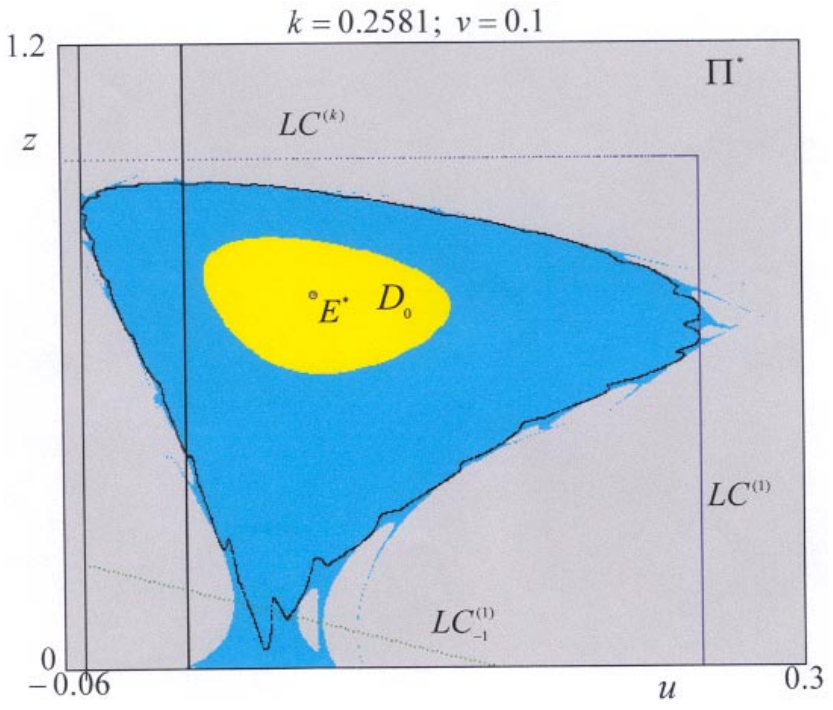

(b)

Fig. 11. Complex dynamics at $v = 0.1$ (a) The repelling invariant curve Γ_u intersects the z-axis. In the enlargement of the basin of attraction of E^* we observe, as a consequence, that the feasible region F_u is smaller than the immediate basin D_0. The boundary of F_u is a portion of the stable set of Γ_u. (b) The folding phenomena on Γ_s, due to the crossing with $LC^{(1)}_{-1}$, are more evident. In this example, the boundary of F_u is still Γ_u. (c) Before the Neimark–Hopf bifurcation, the curve Γ_s has a contact with the boundary of the set S_u and it disappears. Then the Cournot equilibrium E^* is the unique attracting set of the map and its immediate basin coincides with the feasible region F_u. After the Neimark–Hopf bifurcation the generic trajectory is nonadmissible.

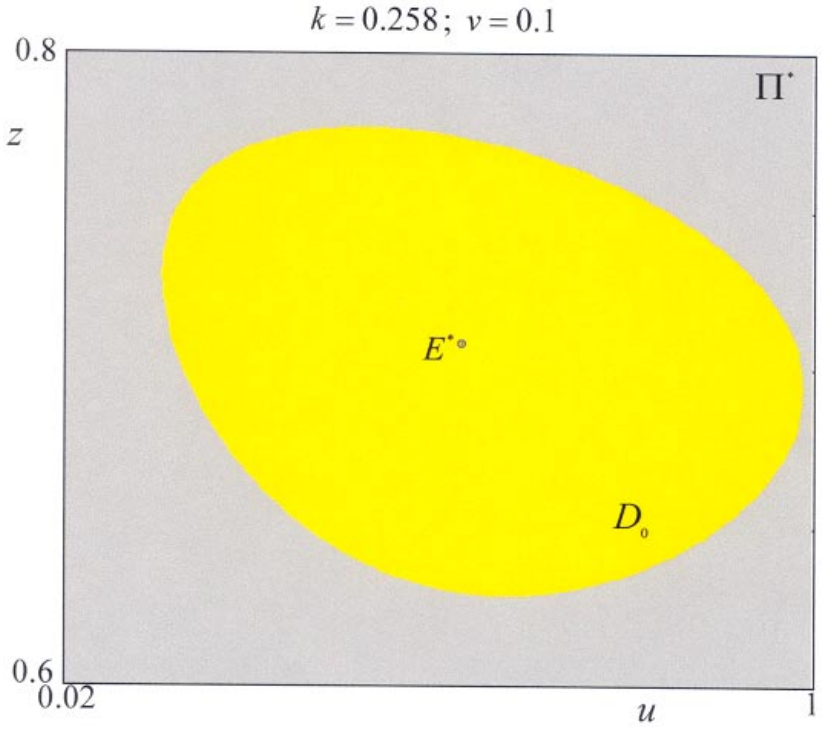

(c)

Fig. 11. (*Continued*)

$k < k_{\text{bif}}^{0.06}$, there are no generic feasible trajectories, because the unique attractor is the closed curve Γ_s. In Fig. 10(b), representing an enlargement of the set S_u, Γ_s shows some "oscillations" in its geometrical shape. This is due to the nonlinearity properties of the map T_u: in fact the curve crosses $LC_{-1}^{(1)}$ causing the folding of Γ_s occurring on $LC^{(1)}$. Moreover Γ_s, in this example, is very close to the boundary of S_u. As the parameter k is further decreased no admissible trajectories appear and the generic trajectory is nonadmissible: the contact between the attractor and the boundary of the set S_u of admissible trajectories may be read as a "final bifurcation".

A different behavior can be observed at $v = 0.1$: in fact, just after the "saddle node type" bifurcation, in Fig. 11(a), the stable closed curve Γ_s and the repelling closed curve Γ_u are not contained in the feasible region F_u, and unfeasible trajectories converging to the fixed point E^* are visible (red points). Now the boundary of the set $D_0 \cap F_u$ is a portion of the stable set of Γ_u. Moreover, before its disappearance, in the attractive curve Γ_s the folding phenomena previously described are more evident, see Fig. 11(b) where Γ_u is now the boundary $\partial\mathcal{B}(E^*)$. From Fig. 11(c), we deduce that the contact of the "chaotic" attractor with the frontier of S_u occurs at $\tilde{k} < k_{\text{bif}}^{0.1}$. Thus, for k in the range $(\tilde{k}, k_{\text{bif}}^{0.1})$, the Cournot equilibrium point is the unique attractor, but its basin of attraction, made up of D_0 and its preimages, is very small, as well as the set of feasible trajectories, coincident with D_0. After the Neimark–Hopf bifurcation the generic trajectory is nonadmissible.

7. The Map T in the Generic Case

Let us return to the 3D map T in the generic case, i.e. we consider the map given in (7), with $k < h < 1$.

In Sec. 3.1 we presented some results about this model, in particular related to the feasibility of the Cournot equilibrium point and its local stability analysis. Now we shall present some global properties of (7), proceeding as in the previous sections for the case $h = 1$, i.e. we shall study the feasible region and some of its bifurcations and analyze the crossing of the bifurcation curve shown in Fig. 1.

First of all, we need to know the Riemann foliation induced by the map and the critical surfaces. We have

Proposition 5. *In the admissible region S, the points (x, y, z) such that*

(a) *$x > 1/4$ or $y > 1/4h$ or $z > 1/4k$ have no preimages, i.e. they belong to Z_0;*
(b) *$x < 0$ and $y < 0$ and $z < 0$ have 1 rank-1 preimage, i.e. they belong to Z_1;*
(c) *$x < 0$ and $y < 0$ and $0 \le z < 1/4k$, or $x < 0$ and $0 \le y < 1/4h$ and $z < 0$ or $0 \le x < 1/4$ and $y < 0$ and $z < 0$ have two distinct rank-1 preimages, i.e. they belong to Z_2;*
(d) *$x < 0$ and $0 \le y < 1/4h$ and $0 \le z < 1/4k$ or $0 \le x < 1/4$ and $y < 0$ and $0 \le z < 1/4k$ or $0 \le x < 1/4h$ and $0 \le y < 1/4h$ and $z < 0$ have four distinct rank-1 preimages, i.e. they belong to Z_4;*
(e) *$0 \le x < 1/4$ and $0 \le y < 1/4h$ and $0 \le z < 1/4k$ have eight distinct rank-1 preimages, i.e. they belong to Z_8.*

The planes $x = 1/4$, $y = 1/4h$ and $z = 1/4k$ are the *Critical Surfaces*, loci of points with two merging preimages, and in the following denoted by $CS^{(1)}$, $CS^{(h)}$ and $CS^{(k)}$, respectively. As we have seen in the previous section, the coordinate planes separate regions of points with a different number of preimages but they do not have merging preimages.

The preimages of the critical planes, *critical set of rank-0,* are given by

$$\begin{aligned} SC_{-1}^{(1)} &: \left\{ y + z = \frac{1}{4} - v \right\} \cap D \\ SC_{-1}^{(h)} &= \left\{ x + z = \frac{1}{4h} - v \right\} \cap D \\ SC_{-1}^{(k)} &: \left\{ x + y = \frac{1}{4k} - v \right\} \cap D \end{aligned} \tag{20}$$

The critical surfaces of rank-0 intersect at the point

$$Q_{-1} = \left(\frac{1}{8}\left(\frac{1}{k} + \frac{1}{h} - 1 - 4v \right), \frac{1}{8}\left(\frac{1}{k} - \frac{1}{h} + 1 - 4v \right), \frac{1}{8}\left(\frac{1}{h} - \frac{1}{k} + 1 - 4v \right) \right)$$

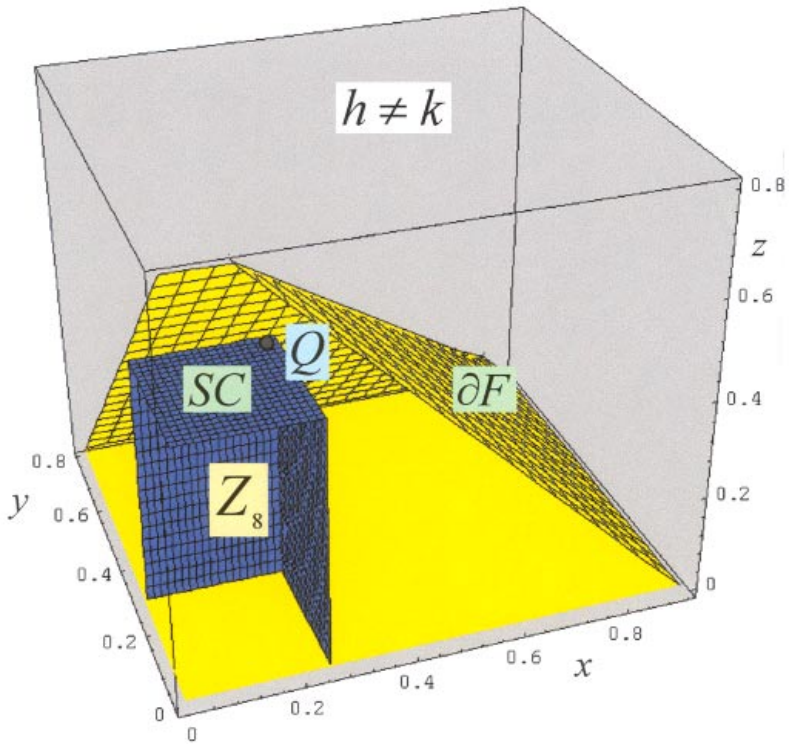

(a)

Fig. 12. Global bifurcation of the feasible region in the case of different producers. (a) The feasible region F is bounded by the coordinate planes and the rank-1 preimages of $x = 0$ and $y = 0$. The critical surfaces are also shown. Q is the intersection point of the critical planes. (b) The rank-1 preimages of $z = 0$ enter the feasible region, truncating the "old" set F. (c) After the contact bifurcation, a volume H of nonadmissible points enters the Z_8 region.

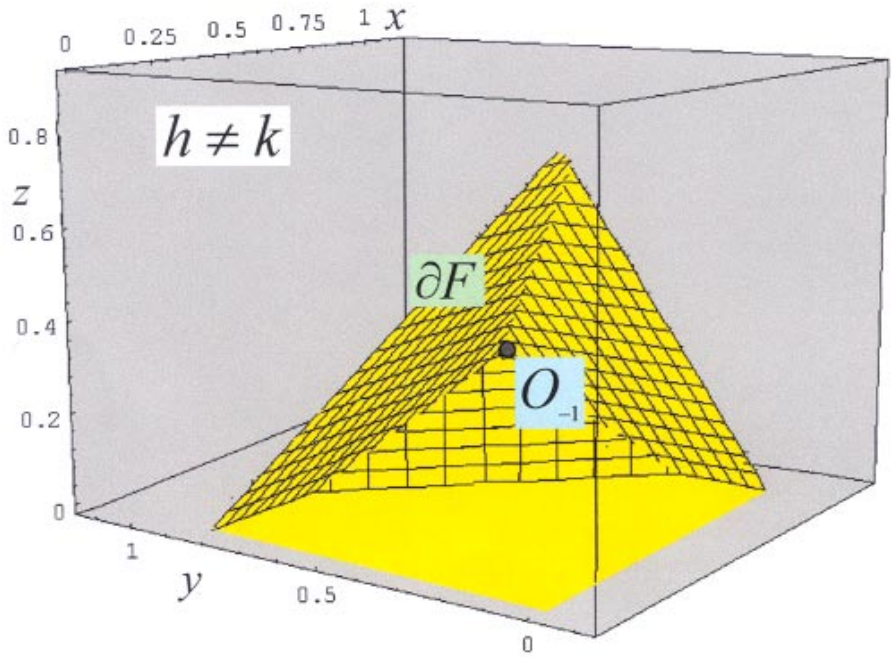

(b)

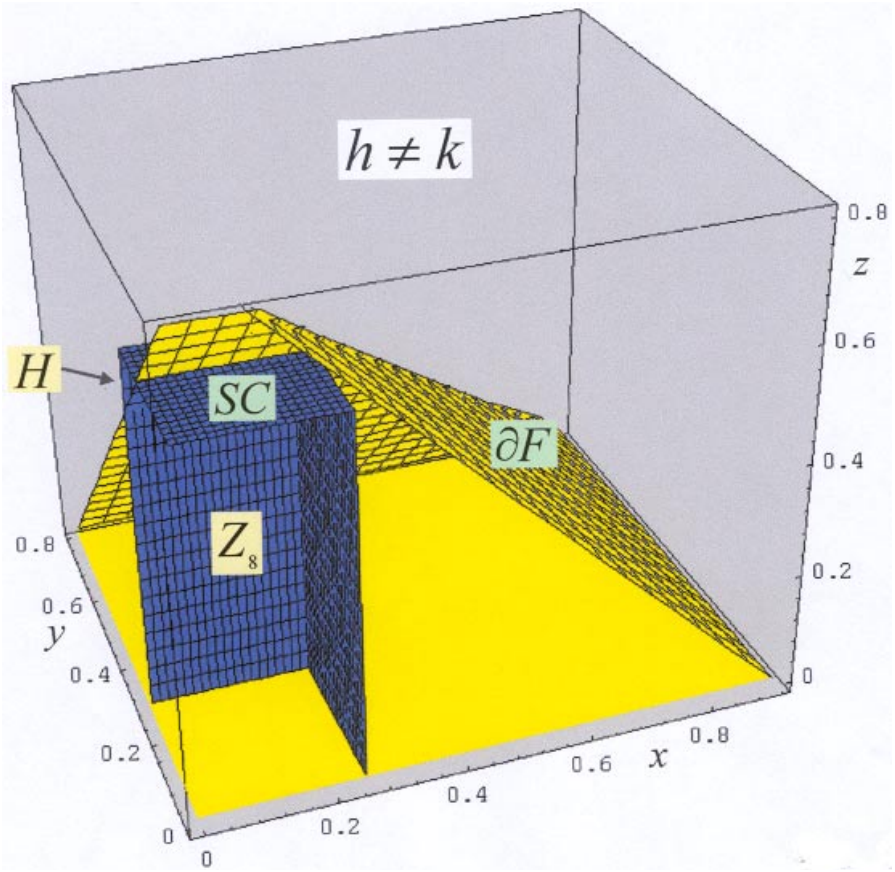

(c)

Fig. 12. (*Continued*)

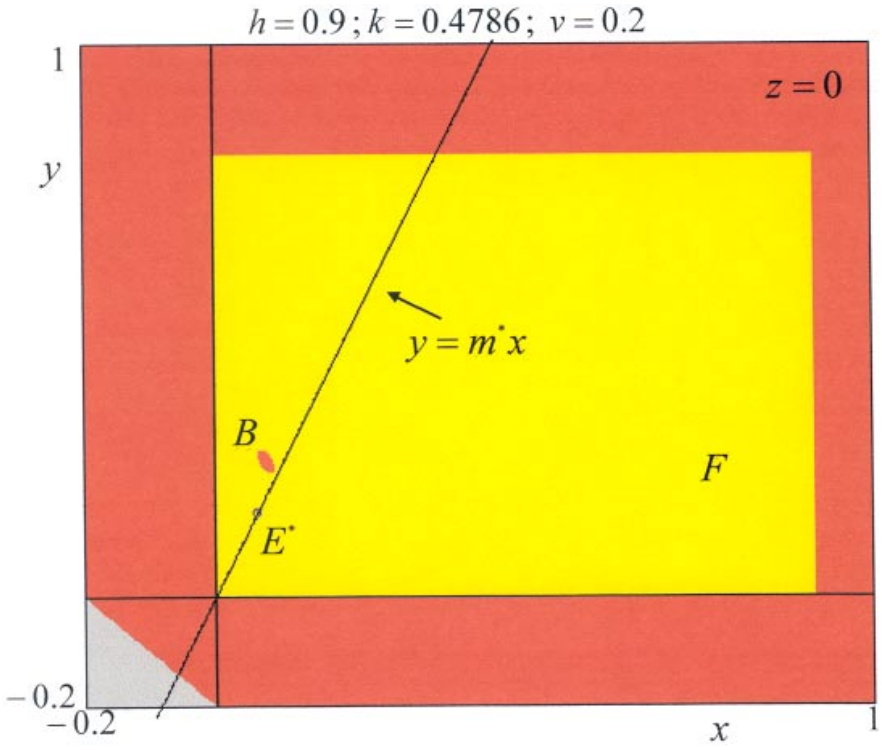

(a)

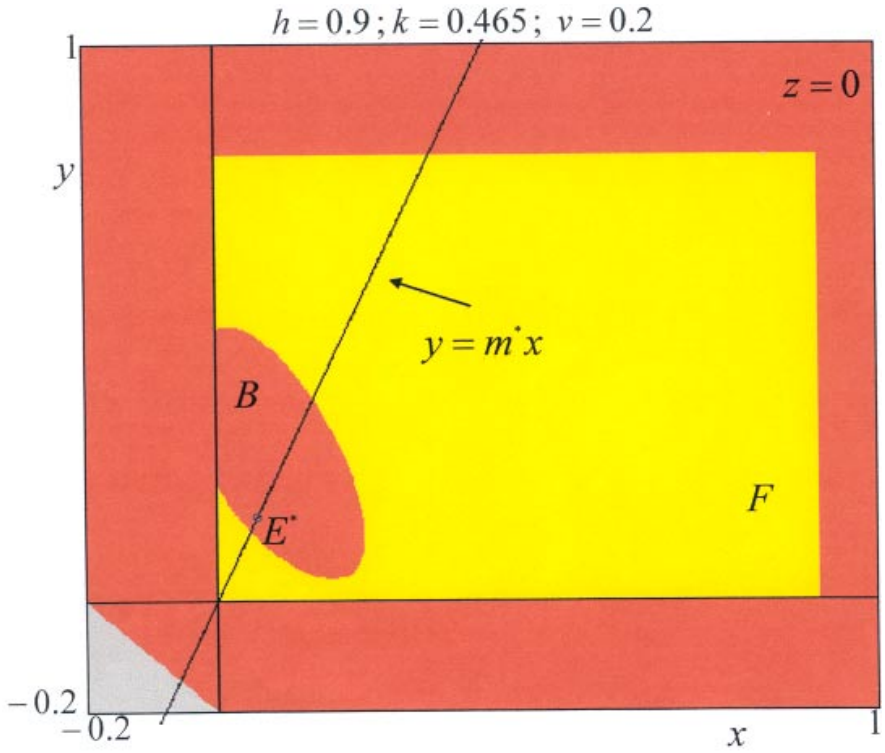

(b)

Fig. 13. (a) The plane section of F with the plane $z = 0$ shows the small red "ball" B of nonadmissible points appearing soon after the contact bifurcation inside the yellow set. (b and c) As the value of k decreases, this "ball" increases in size. (d) A different plane section of F. The plane considered has equation $y = m^*x$ and includes the fixed point.

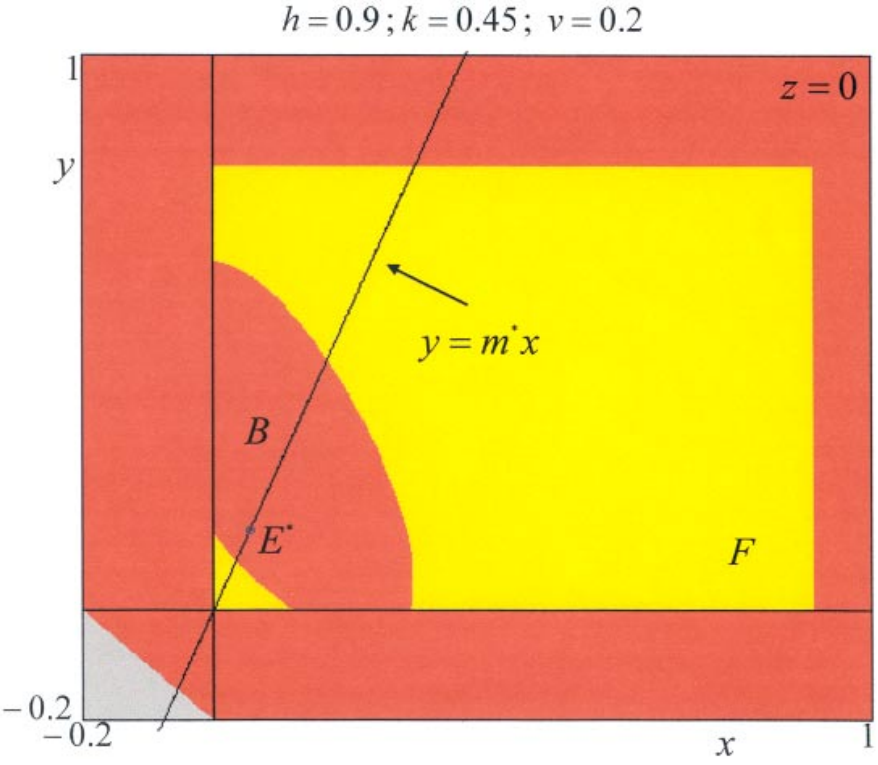

(c)

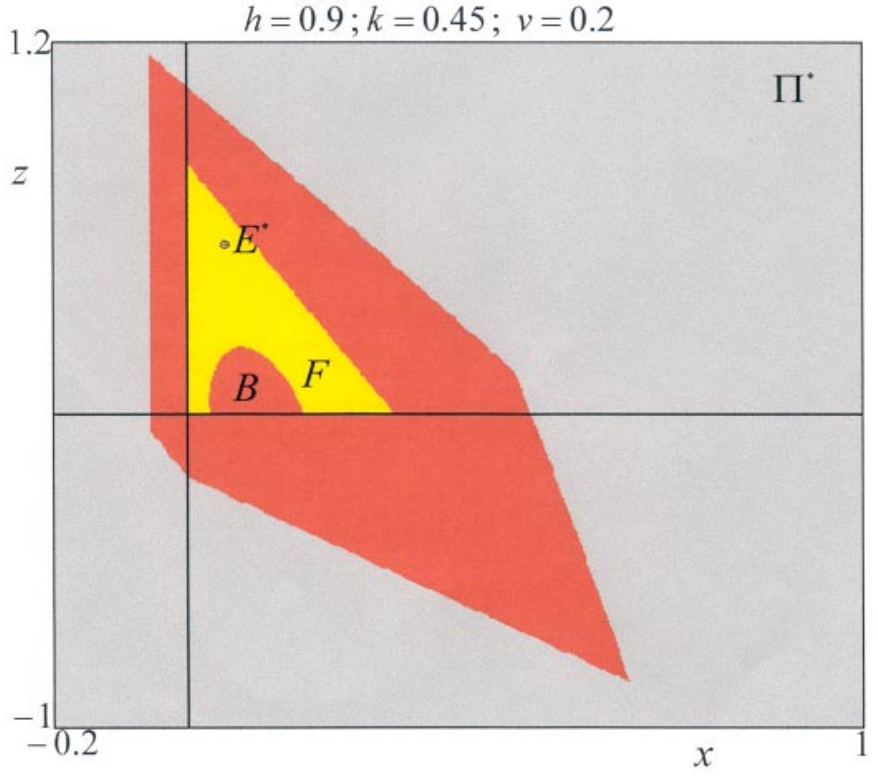

(d)

Fig. 13. (*Continued*)

rank-1 preimage of $Q = (1/4, 1/4h, 1/4k)$, which has eight coincident preimages in Q_{-1}.

We start our analysis with a low value of v, $v = 0.2$, and we set h and k so that the fixed point E^* is an attractor in the feasible region F. As in the previous case, three different shapes for F can be found. The simpler case is shown in Fig. 12(a) in which F is the connected volume bounded by the coordinate planes and by the planes $y+z = 1-v$, preimage of rank-1 of $\{x = 0\}\cap Z_8$, and $x+z = 1/h-v$, preimage of rank-1 of $\{y = 0\}\cap Z_8$: once more the producer with lowest marginal cost has the opportunity to expel the competitors of the market, and to fix a monopoly price. In Fig. 12(a) the region Z_8, bounded by the critical surfaces and the coordinate plane is shown. As we have already seen in Sec. 5 the region F may undergo several kinds of global bifurcations. One is related to the preimage of rank-1 of the region $\{z = 0\} \cap Z_8$, i.e. $x + y = (1/k) - v$. In fact, when the relation

$$1 + \frac{1}{h} - \frac{1}{k} - v \geq 0 \tag{21}$$

holds, then even the opportunities of the third producer are reduced and the region F is bounded by the preimages of the third coordinate plane $\{z = 0\} \cap Z_8$ which modifies the "back" of the feasible region, as qualitatively shown in Fig. 12(b), which corresponds to the "truncated pyramid" of Sec. 5.2. Condition (21) can be obtained observing that the three preimages of the coordinate planes intersect at the point

$$O_{-1} = \left(\frac{1}{k} + \frac{1}{h} - 1 - v,\ \frac{1}{k} - \frac{1}{h} + 1 - v,\right.$$
$$\left. - \frac{1}{k} + \frac{1}{h} + 1 - v\right)$$

one of the preimages of the point $O = (0, 0, 0)$, and $O_{-1} \in R^3_+$ iff (21) holds. We remark that (21) is equivalent to say that the z-coordinate of O_{-1} is positive, whereas the other two coordinates are always positive, being $(1/k)+(1/h)-1-v > 1-v > 0$ and $(1/k)-(1/h)+1-v > 0$ in the range of interest of the parameters.

A second global bifurcation of F occurring is a *contact bifurcation*, due to the contact of the critical surfaces with the preimages of the coordinate plane, constituting ∂F. An example is shown in Fig. 12(c), where the contact has just occurred and a portion of the region Z_8 which is now in the unfeasible region is clearly evident. The bifurcation value is given by

$$k = \frac{h}{4(1-v)h - 1}$$

obtained by the condition that the vertex Q belongs to the plane $y + z = 1 - v$. The effect of this second bifurcation is the creation of a volume of unfeasible region inside the feasible one, due to the preimages of the portion of Z_8 which is now (after the contact) located in the unfeasible region. This is illustrated in Fig. 13, where some sections of the three-dimensional space are drawn. In Fig. 13(a) we can see the small red "ball" inside the feasible yellow region, appeared soon after the contact bifurcation, as the section of the "ball" on the plane $z = 0$. On decreasing the value of the parameter k, this "ball" increases in size, as we can see from the sections in Figs. 13(b) and 13(c). In Fig. 13(d) we show the section of the feasible three-dimensional region taken on a different plane, of equation $y = mx$ including the fixed point, say Π^*. The three-dimensional feasible region illustrated in Fig. 13 is always a connected set and its origin and bifurcations are similar to those already described in the previous sections. The "ball" is located around the point Q_{-1} and, due to the lack of symmetry between the producers, it is not symmetric with respect to the plane Π^*.

Also the crossing of the bifurcation curve, for low values of v, gives rise to situations similar to the ones analyzed in Sec. 6. In particular, the effect of the saddle-node type bifurcation, which gives rise to the appearance of two closed invariant curves, one attracting (Γ_s) and the other repelling (Γ_u). The stable set of Γ_u constitutes the boundary of the basin of the equilibrium point E^*, which is feasible if Γ_u belongs to the positive orthant of the space. As the parameter values approach the bifurcation curve, the curve Γ_u becomes smaller and smaller and, at the bifurcation values, it shrinks on E^*, which becomes unstable (Neimark–Hopf bifurcation of subcritical type).

Acknowledgment

This work has been performed as part of the national research project "Dynamic Models in Economics and Finance", MURST, Italy.

References

Abraham, R., Gardini, L. & Mira, C. [1997] *Discrete Dynamical Systems in Two Dimensions* (Springer-Verlag, Berlin).

Agliari, A., Gardini, L. & Puu, T. [2000] "The dynamic of a triopoly Cournot game," *Chaos Solit. Fract.* **11**, 2531–2560.

Bertrand, J. [1883] "Théorie mathématique de la Richesse sociale," *J. des Savants* **48**, 499–508.

Binmore, K. [1992] *Fun and Game* (Heath, Lexington Mass).

Cournot, A. [1838] *Récherches sur les Principes Mathématiques de la Théorie des Richesses* (Hachette, Paris).

Edgeworth, F. Y. [1897] "La teoria pura del monopolio," *Giornale degli Economisti* **15**, 13–31.

Fellner, W. [1949] *Competition Among the Few — Oligopoly and Similar Market Structures* (Alfred A. Knopf, NY).

Friedman, J. [1983] *Oligopoly Theory* (Cambridge University Press).

Frisch, R. [1933] "Monopole – Polypole – La notion de force dans l'économie," *Nationaloekonomisk Tidsskrift* **71**, 241–259.

Gumonwski, I. & Mira, C. [1980a] *Dynamique Chaotique. Transition Ordre-desordre* (Cepadues, Toulouse).

Gumonwski, I. & Mira, C. [1980b] *Recurrences and Discrete Dynamic Systems*, Lectures Notes in Mathematics, Vol. 809 (Springer-Verlag, Berlin).

Mira, C., Gardini, L., Barugola, A. & Cathala, J. C. [1996] *Chaotic Dynamics in Two-dimensional Noninvertible Maps* (World Scientific, Singapore).

Palander, T. [1936] "Instability in competition between two sellers," in *Abstracts of Papers Presented at the Research Conf. Economics and Statistics*, Cowles Commission at Colorado College, Colorado College Publications, General Series No. 208, Studies Series No. 21.

Puu, T. [1991] "Chaos in duopoly pricing," *Chaos Solit. Fract.* **1**, 573–581.

Puu, T. [2000] *Attractors, Bifurcations & Chaos-Nonlinear Phenomena in Economics* (Springer-Verlag).

Rand, D. [1978] "Exotic phenomena in games and duopoly models," *J. Math. Econ.* **5**, 173–184.

von Stackelberg, H. [1938] "Probleme der unvollkommenen Konkurrenz," *Weltwirtschaftliches Archiv* **48**, 95–114.

Wald, A. [1936] "Über einige gleichungssysteme der mathematischen ökonomie," *Zeitschrift für Nationalökonomie* **7**, 637–670.

Appendix A
Reaction Functions

Let us consider the game G in normal form given by

$$G = \{I, S, U\}$$

where

- $I = \{1, 2, \ldots, n\}$ is the set of players;
- $S = S_1 \times S_2 \times \cdots \times S_n$ is the set of the *strategic profiles* of the game and S_i is the set of *strategies* of the ith player;
- U is the *payoff*, i.e. the function $U : S \to R^n$ such that $U_i(s)$ is the *utility* of the ith player corresponding to the strategic profile s.

Observe that the utility of each player depends on his strategy but also on that of his competitors. Then, in order to choose the "best action", each player has to know the moves of the other players.

In the game G, the *best response correspondence* of a player is defined as the set of its strategies which give him the best result, in term of utility, if used as a reply to the moves of the competitors, see [Binmore, 1992].

More formally

$$r_i(s_{-i}) = \arg \max_{s_i \in S_i} U_i(s_i, s_{-i})$$

where s_{-i} is the strategic profile of the competitors of player i, i.e.

$$s_{-i} = (s_1, \ldots, s_{i-1}, s_{i+1}, \ldots, s_n)$$

Generally $r_i : S_{-i} \to S_i$ is a correspondence one-to-many, but, when $u_i(s)$ is a unimodal function of s_i, then r_i is a function and it is called *reaction function*.

This is the case of the Cournot model considered in the present paper. In fact, it can be considered as a game G in which $I = \{1, 2, 3\}$, $S = \{(x, y, z) : x \geq 0, y \geq 0, z \geq 0\}$ is the set of the quantities and $U = (U_1, U_2, U_3)$, where the functions U_i are given in (2).

Let us fix our attention on player 1, with marginal cost a. We have

$$\frac{\partial U_1}{\partial x} = \frac{y + z + W}{(x + y + z + W)^2} - a$$

and, U_1 being a concave function in x, the reaction function is

$$r_1(y, z) = \arg \max_x U_1 = \sqrt{\frac{y + z + W}{a}} - y - z - W$$

In an analogous way, $r_2(x, z)$ and $r_3(x, y)$ are obtained as given in (3).

Given the best response correspondence for each player, we can consider $R : S \to S$ such that

$$R_i(s) = r_i(s_{-i})$$

The fixed points of R, when exist, are the *Nash equilibria* of the game (*Cournot points* in oligopoly theory), i.e. the strategic profiles s^* such that

$$\forall\, i \in I \quad \forall\, \tilde{s} \in S_i \quad u_i(s^*) \geq u_i(\tilde{s},\, s^*_{-i})$$

Appendix B
Proof of Proposition 3

Proof. The positivity of the coordinates of E^*_u can be obtained by Proposition 2, considering $h = 1$. The stability condition is obtained in the usual way, considering the Jacobian matrix of T_u in the fixed point:

$$J^*_u = \begin{bmatrix} \dfrac{2+k}{2(1+\sqrt{1+v(2+k)})} - 1 & \dfrac{2+k}{2(1+\sqrt{1+v(2+k)})} - 1 \\ \dfrac{2+k}{k(1+\sqrt{1+v(2+k)})} - 2 & 0 \end{bmatrix}$$

We have $\mathrm{trace}(J^*_u) = 2 + k/(2+2\sqrt{1+v(2+k)}) - 1$ and

$$\det(J^*_u) = -\left(\frac{2+k}{2+2\sqrt{1+v(2+k)}} - 1\right) \times \left(\frac{2+k}{k(1+\sqrt{1+v(2+k)})} - 2\right),$$

so that the well-known stability conditions give

$1 - \mathrm{trace}(J^*_u) + \det(J^*_u) > 0$ which is true for every k and v as it reads:

$$\frac{1}{2}\sqrt{1+v(2+k)}\,\frac{(2+k)^2}{(1+\sqrt{1+v(2+k)})^2 k} > 0\,.$$

$1 + \mathrm{trace}(J^*_u) + \det(J^*_u) > 0$ reads:

$$\frac{2k^2 + 3k^2\sqrt{1+v(2+k)} + 4\sqrt{1+v(2+k)} \quad -4k - 8vk - 4vk^2}{2k(1+\sqrt{1+v(2+k)})^2} > 0$$

and this inequality is true in the range of interest of the parameters because

$$\begin{aligned} 2k^2 + 3k^2\sqrt{1+(2+k)v} + 4\sqrt{1+(2+k)v} - 4k - 8vk - 4vk^2 &\geq 2k^2 + 3k^2 + 4 - 4k - 8vk - 4vk^2 \\ &= 5k^2 + 4 - 4k - 8vk - 4vk^2 \\ &= 4k^2 + (k+2)^2 - 4vk(k+2) \\ &\geq 4k^2 + (k+2)^2 - 4k(k+2) \\ &= (k-2)^2 \end{aligned}$$

where the first inequality follows by $\sqrt{1+(2+k)v} \geq 1$ and the second by $v \leq 1$.

Finally

$$\det(J^*_u) = -\left(\frac{2+k}{2+2\sqrt{1+v(2+k)}} - 1\right) \times \left(\frac{2+k}{k(1+\sqrt{1+v(2+k)})} - 2\right) < 1$$

reduces to the inequality

$$2(2-k)(1-k)\sqrt{1+v(2+k)} < 6vk(k+2) + k(10-k)$$

and, being $k \leq 1$, to

$$36k^2v^2 - 4v(k^3 - 5k^2 - 7k + 2) - 36k^2 + 16k - 4 > 0$$

whose solutions are

- $0 < k < (8 - 2\sqrt{13})/3$, $v > [k^3 - 5k^2 - 7k + 2 + (1-k)(2-k)\sqrt{k^2 - 4k + 1}]/18k^2$
- $k \geq (8 - 2\sqrt{13})/3$, any v.

■